International Journal of Bifurcation and Chaos

Hopf and Generalized Hopf bifurcations in a Recurrent Autoimmune Disease Model

WENJING ZHANG [a], and PEI YU [b*]

[a] *Department of Mathematics and Statistics, York University, Toronto, Ontario, M3J 1P3, Canada*
[b] *Department of Applied Mathematics, Western University London, Ontario, N6A 5B7, Canada*

Received (to be inserted by publisher)

This paper is concerned with bifurcation and stability in an autoimmune model, which was established to study an important phenomenon – blips arising from such models. This model has two equilibrium solutions, disease-free equilibrium and disease equilibrium. The positivity of the solutions of the model and the global stability of the disease-free equilibrium have been proved. In this paper we particularly focus on Hopf bifurcation which occurs from the disease equilibrium. We present a detailed study on the use of center manifold theory and normal form theory, and derive the normal form associated with Hopf bifurcation, from which approximate amplitude of the bifurcating limit cycles and their stability conditions are obtained. Numerical simulations are compared with the analytical predictions to show a very good agreement.

Keywords: Autoimmune disease model, stability, Hopf bifurcation, Limit cycle, Center manifold, Normal form.

1. Introduction

Autoimmune diseases arise from an inappropriate immune system in responding against its own cells and tissues, which are normally present in the body. A substantial minority of population, approximately 3% of people in "developed" countries, suffer from over 40 recognized autoimmune diseases [DeFranco *et al.*, 2007], which are often chronic, depleting and fatal. While some autoimmune diseases show recurrent (or blips) behavior, which was found typically in multifocal osteomyelitis [Girschick *et al.*, 2007; Iyer *et al.*, 2011], Eczema [Fergusson it et al., 1990], subacute discoid lupus erythematosus [Munro, 1963], and psoriasis [Mullen *et al.*, 1986]. During the recurrent autoimmune disease, the disease symptoms can disappear spontaneously, but it will be occasionally replase later. Therefore, a profound study on the recurrent dynamics of autoimmune disease is important to obtain a broad understanding of this disease phenomenon.

In immune system, regulatory T (Treg) cells, a subpopulation of T cells, play a crucial role in tolerance to the body's own cells and tissues, and suppress autoimmune response. Treg cells operate primarily at the site of inflammation. The mechanisms for Treg cells modulating the immune reaction is one of the most intensely studied and debated issues, while "there might be a single key mechanism that has a predominant role", as Miyara and Sakaguchi pointed out in [Miyara and S. Sakaguchi, 2007]. Here, we adopt two mechanisms proposed in a general autoimmune disease model by Alexander and Wahl [Alexander &

*wzhan88@yorku.ca (W. Zhang), pyu@uwo.ca (P. Yu, corresponding author).

Wahl, 2011]. One mechanism is that Treg cells act suppression directly on professional antigen presenting cells (pAPCs), which play a vital role in activating naive T cells, and remove pAPCs permanently. The other mechanism is that the Treg cells directly reduce and remove the peripheral auto-reactive effector T cells, which have antigen receptors specific to self-antigens and ready to attack host cells. Phenotypic analysis shows that Treg cells subset is heterogeneous [Sakaguchi *et al.*, 2010] in the expression of HLA-DR, which identifies a terminally differentiated subpopulation of Treg cells with HLA-DR$^+$, called terminal Treg cells. The terminal Treg cells are generated from natural Treg cells proliferation [Sakaguchi *et al.*, 2010], while suppress more efficiently and tend to be apoptotic much faster than the natural Treg cells. The following mathematical model was established to model the Treg cells activity in modulating immune response [Zhang *et al.*, 2014],

$$\begin{aligned}
\dot{A} &= \alpha E - \sigma_1(R_n + dR_d)A - b_1 A - \mu_A A,\\
\dot{R}_n &= (\pi_3 E + \beta)A - \mu_n R_n - \xi R_n,\\
\dot{R}_d &= c\,\xi R_n - \mu_d R_d,\\
\dot{E} &= \lambda_E A - \sigma_3(R_n + dR_d)E - b_3 E - \mu_E E.
\end{aligned} \tag{1}$$

where the state variables A, R_n, R_d and E represent the population of the mature pAPCs, the activated natural Treg cells specific for antigen of interest, terminally differentiated Treg cells, and the active auto-reactive effector T cells with specific antigen of interest. The pAPCs are activated at a rate of $\alpha\,E$ by uptaking self-antigen, which is generated by effector T cells attacking body cells, The relation between effector T cells and self-antigen is linear under quasi-steady state assumption. The pAPCs are suppressed by the Treg cells with specific antigen of interest at a rate of $\sigma_1\,(R_n + d\,R_d)\,A$, where d is the ratio of suppressive effectiveness between the natural Treg cells and terminally differentiated Treg cells, while the Treg cells with other specificities and therapy can also suppress pAPCs at a rate of b_1. The natural Treg cells are activated with interaction of the pAPCs in the presence of IL-2 which is generated by the effector T cells at a rate of $\pi_3\,E$, and by other sources like dendritic cells (DCs) [Field *et al.*, 2007; Scheffold *et al.*, 2005, 2007] at a rate of β, and thus the natural Treg cells generation rate is $(\pi_3\,E + \beta)\,A$. The activated natural Treg cells may undergo further differentiation and proliferation [Sakaguchi *et al.*, 2010] at a rate of ξ and give birth to terminally differentiated Treg cells at a rate of $c\,\xi\,R_n$. The vicious effector T cells are activated by the pAPCs bearing a specific antigen receptor, at a rate of $\lambda_E\,A$, and are suppressed by the Treg cells with specific antigen of interest at a rate of $\sigma_3\,(R_n + d\,R_d)\,E$, and the Treg cells with other specifities and therapy at a rate of $b_3\,E$. The death rates of the pAPCs, natural Treg cells, terminally differentiated Treg cells, and effector T cells are μ_A, μ_n, μ_d, and μ_E, respectively.

It has been shown in [Zhang *et al.*, 2014] that all solutions of (1) are non-negative, if the initial conditions are taken non-negative, and they are bounded. Moreover, a detailed analysis on the stability of equilibrium solutions is also given in [Zhang *et al.*, 2014]. Thus, in this paper, we will focus on nonlinear study of model (1), in particular on Hopf and generalized Hopf bifurcations, giving rise to multiple limit cycles bifurcating from the disease equilibrium solution. The rest of the paper is organized as follows. In the next section, we provide a brief summary on he linear analysis of system (1), and find the transcritical and Hopf bifurcations from the equilibrium solutions. Then, in Section 3, we devote to nonlinear analysis and focus on Hopf bifurcation. Center manifold theory and normal form theory will be used to find the approximate solution of limit cycles and determine their stability. In Section 4, we give a study on generalized Hopf bifurcation, showing that at least two small-amplitude limit cycles can bifurcate from the disease equilibrium solution. Numerical simulations are given in Section 5 to show the good agreement between simulations and analytical predictions. Finally, conclusion is drawn in Section 6.

2. Equilibrium solutions, stability and bifurcation: Linear analysis

In order to consider stability of equilibrium solutions of model (1), we first present certain results and formulas for general systems. Consider the general nonlinear differential system:

$$\dot{\mathbf{x}} = \mathbf{f}(\mathbf{x}, \boldsymbol{\mu}), \quad \mathbf{x} \in \mathbf{R}^n, \quad \boldsymbol{\mu} \in \mathbf{R}^m, \quad \mathbf{f} : \mathbf{R}^{n+m} \mapsto \mathbf{R}^n, \tag{2}$$

where the dot denotes differentiation with respect to time, t; $\mathbf{x}$ and $\boldsymbol{\mu}$ are the n-dimensional state variable and m-dimensional parameter variable, respectively. It is assumed that the nonlinear function $\mathbf{f}(\mathbf{x}, \boldsymbol{\mu})$ is analytic with respect to $\mathbf{x}$ and $\boldsymbol{\mu}$. Suppose that the equilibrium solutions of equation (2) are given in the form of $\mathbf{x}_e = \mathbf{x}_e(\boldsymbol{\mu})$, which are determined from $\mathbf{f}(\mathbf{x}, \boldsymbol{\mu}) = 0$. To find the stability of $\mathbf{x}_e$, evaluating the Jacobian of system (2) at $x = \mathbf{x}_e(\boldsymbol{\mu})$ yields $\mathbf{J}(\boldsymbol{\mu}) = D_{\mathbf{x}}\mathbf{f}|_{x=\mathbf{x}_e(\boldsymbol{\mu})}$. If all eigenvalues of $\mathbf{J}(\boldsymbol{\mu})$ have nonzero real parts, then the system is said to be hyperbolic and no complex dynamics exists in the vicinity of the equilibrium solution. If at some point $\boldsymbol{\mu} = \boldsymbol{\mu}_c$, at least one of the eigenvalues of $\mathbf{J}(\boldsymbol{\mu})$ has zero real part, then $\boldsymbol{\mu}_c$ is called a critical point, and bifurcation may occur from $\mathbf{x}_e(\boldsymbol{\mu})$. To determine the stability of the equilibrium solution, we need to find the eigenvalues of the Jacobian $\mathbf{J}(\boldsymbol{\mu})$, which are the roots of the following polynomial equation:

$$P_n(L) = \det[L\,I - \mathbf{J}(\boldsymbol{\mu})] = L^n + a_1(\boldsymbol{\mu})L^{n-1} + a_2(\boldsymbol{\mu})L^{n-2} + \cdots + a_{n-1}(\boldsymbol{\mu})L + a_n(\boldsymbol{\mu}) = 0. \tag{3}$$

If for a value of $\boldsymbol{\mu}$, all the roots of the polynomial $P_n(L)$ have negative real part, then the equilibrium solution is asymptotically stable for this value of $\boldsymbol{\mu}$. If at least one of the eigenvalues has zero real part as $\boldsymbol{\mu}$ crosses a critical point, $\boldsymbol{\mu}_c$, then the equilibrium solution becomes unstable at $\boldsymbol{\mu}_c$ and bifurcation occurs from this critical point. When all the roots of $P_n(L)$ have negative real part, we call $P_n(L)$ a *stable polynomial*, otherwise an *unstable polynomial.*

In general, for $n \geq 3$, it is hard or impossible to find the roots of $P_n(L)$. Thus we use the Routh-Hurwitz criterion [Hinrichsen & Pritchard, 2005] to analyze the local stability of the equilibrium solution $x = \mathbf{x}_e(\boldsymbol{\mu})$. The criterion states that the necessary and sufficient conditions, under which the corresponding equilibrium is locally asymptotically stable, i.e. all the roots of the polynomial $P_n(L) = 0$ in equation (3) have negative real part, are given by

$$\Delta_i(\boldsymbol{\mu}) > 0, \quad i = 1, 2, \ldots, n, \tag{4}$$

where $\Delta_i(\boldsymbol{\mu})$ are called the ith-principal minors of the Hurwitz arrangements of *order* n, defined as follows (here, *order* n means that there are n coefficients, a_i $(i = 1, 2, \ldots, n)$ in equation (3), which construct the Hurwitz principal minors):

$$\Delta_1 = a_1, \quad \Delta_2 = \det\begin{bmatrix} a_1 & 1 \\ a_3 & a_2 \end{bmatrix}, \quad \Delta_3 = \det\begin{bmatrix} a_1 & 1 & 0 \\ a_3 & a_2 & a_1 \\ a_5 & a_4 & a_3 \end{bmatrix}, \quad \ldots, \quad \Delta_n = a_n\Delta_{n-1}. \tag{5}$$

Suppose as $\boldsymbol{\mu}$ is varied to reach a critical point, $\boldsymbol{\mu} = \boldsymbol{\mu}_c$, at least one of Δ_i's becomes zero, then the fixed point $\mathbf{x}_e(\boldsymbol{\mu}_c)$ becomes unstable, and $\boldsymbol{\mu}_c$ is called critical point. It is easy to see from equation (3) that if $a_n(\boldsymbol{\mu}) = 0$ (then $\Delta_n = 0$), but other Hurwitz arrangements are still positive (i.e. $\Delta_i(\boldsymbol{\mu}) > 0, \quad i = 1, 2, \ldots, (n-1)$), $P_n(L) = 0$ has one zero root, indicating that system (2) has a simple zero singularity and a static bifurcation occurs from $\mathbf{x}_e$. For other complex dynamical behavior, for example, Hopf bifurcation occurs at a critical point at which $P_n(L) = 0$ has a pair of purely imaginary eigenvalues, $\pm i\,\omega\,(\omega > 0)$. But this pair of purely imaginary eigenvalues are often difficult to be determined explicitly for high dimensional systems. Based on the Hurwitz criterion, the following theorem states the necessary and sufficient conditions for determining Hopf critical point without computing the eigenvalues of the Jacobian of the corresponding system. Its proof can be found in [Yu, 2005].

Theorem 1. *[Yu, 2005] The necessary and sufficient conditions for system (2) to have a Hopf bifurcation at an equilibrium solution* $\mathbf{x} = \mathbf{x}_e$ *is* $\Delta_{n-1} = 0$, *with other Hurwitz conditions being still held, i.e.* $a_n > 0$ *and* $\Delta_i > 0$, *for* $i = 1, \ldots, n-2$.

2.1. *Equilibrium solutions*

Having established general results in the previous subsection, we now return to model (1). The equilibrium solutions of this model can be obtained by simply setting $\dot{A} = \dot{R}_n = \dot{R}_a = \dot{E} = 0$ and solving the resulting algebraic equations, which yields two equilibrium solutions: the disease-free equilibrium E_0 and the disease equilibrium E_1. They are given by

$$
\begin{aligned}
&E_0 : (0,\,0,\,0,\,0)\\
&E_1 : \Big(A_1,\ \tfrac{\mu_d[\pi_3(b_1+\mu_A)A_1+\beta\alpha]A_1}{\mu_d\alpha(\mu_n+\xi)-\pi_3\sigma_1(\mu_d+dc\xi)A_1^2},\ \tfrac{c\,\xi\bar{R}_n}{\mu_d},\ \tfrac{[\sigma_1\bar{R}_n(\mu_d+dc\xi)+\mu_d(b_1+\mu_A)]A_1}{\mu_d\alpha}\Big),
\end{aligned}
\tag{6}
$$

where A_1 is given in a function of the system parameters, particularly in α, which is implicitly determined by the following 4th-degree polynomial equation in A_1:

$$
F_1(A_1,\,\alpha) = \tfrac{81}{38146972656250}\,A_1^4 - \tfrac{1521}{625000000}\,\alpha A_1^2 - \tfrac{81}{10000000}\alpha A_1 + \tfrac{5}{8}\alpha^2 - \tfrac{81}{640000}\alpha = 0. \tag{7}
$$

in which the parameter values given in Table 2.1 have been used. Note that the rational numbers given in this equation are obtained using symbolic computation in which all the parameter values given in digital format (see Table 2.1) have been transformed to rational numbers for convenience in computation.

Parameter values used in model (1) [Alexander & Wahl, 2011]

Parameter	Value	Parameter	Value
π_3	0.0256 day^{-1} per E per A (π_3)	β	200 day^{-1}per A
λ_E	1000 day^{-1}per A	b_1	0.25 day^{-1} per E
$\sigma_{1,3}$	3×10^{-6} day^{-1} per R (or R_n or R_d)) per A	b_3	0.25 day^{-1} per E
μ_A	0.2 day^{-1}per A	μ_E	0.2 day^{-1}per E
μ_n	0.1 day^{-1}per R_n	μ_d	0.2 day^{-1}per R_d
ξ	0.025 per R_n	α	Bifurcation parameter
d	2	c	$2^3 = 8$

The graph showing the component A of the equilibrium solutions E_0 and E_1, i.e., $A = 0$ and $A = A_1$ satisfying $F_1(A_1,\,\alpha) = 0$, is given in Figure 1. Note that a complete bifurcation diagram is depicted in Figure 1(a), while its part which has biologically meaning is given in Figure 1(b). In order to display the biological meaningful solutions, a 3-dimensional plotting is shown in Figure 1(c), indicating that one branch of each solution in Figure 1(a) is biologically meaningless.

2.2. *Stability of the equilibria*

For the stability of the disease-free equilibrium E_0, characteristic equation method and Lyapunov function method have been used in [Zhang *et al.*, 2014] to obtain the following result.

Lemma 1. *When $\alpha < \alpha_t = \frac{1}{\lambda_E}(b_1+\mu_A)(b_3+\mu_E)\alpha_t$, the disease-free equilibrium E_0 of model (1) is globally asymptotically stable. It loses stability at $\alpha = \alpha_t$ and becomes unstable for $\alpha > \alpha_t$.*

Next, consider the stability of the disease equilibrium E_1. Evaluating the Jacobian matrix of (1) at E_1 yields a 4th-degree characteristic polynomial, given by

$$
P_1(L, A_1, \alpha) = L^4 + a_1(A_1,\alpha)L^3 + a_2(A_1,\alpha)L^2 + a_3(A_1,\alpha)L + a_4(A_1,\alpha) = 0. \tag{8}
$$

where the coefficients $a_1(A_1,\alpha)$, $a_2(A_1,\alpha)$, $a_3(A_1,\alpha)$, and $a_4(A_1,\alpha)$ are expressed in terms of A_1 and α, with other parameter values taken from Table 2.1.

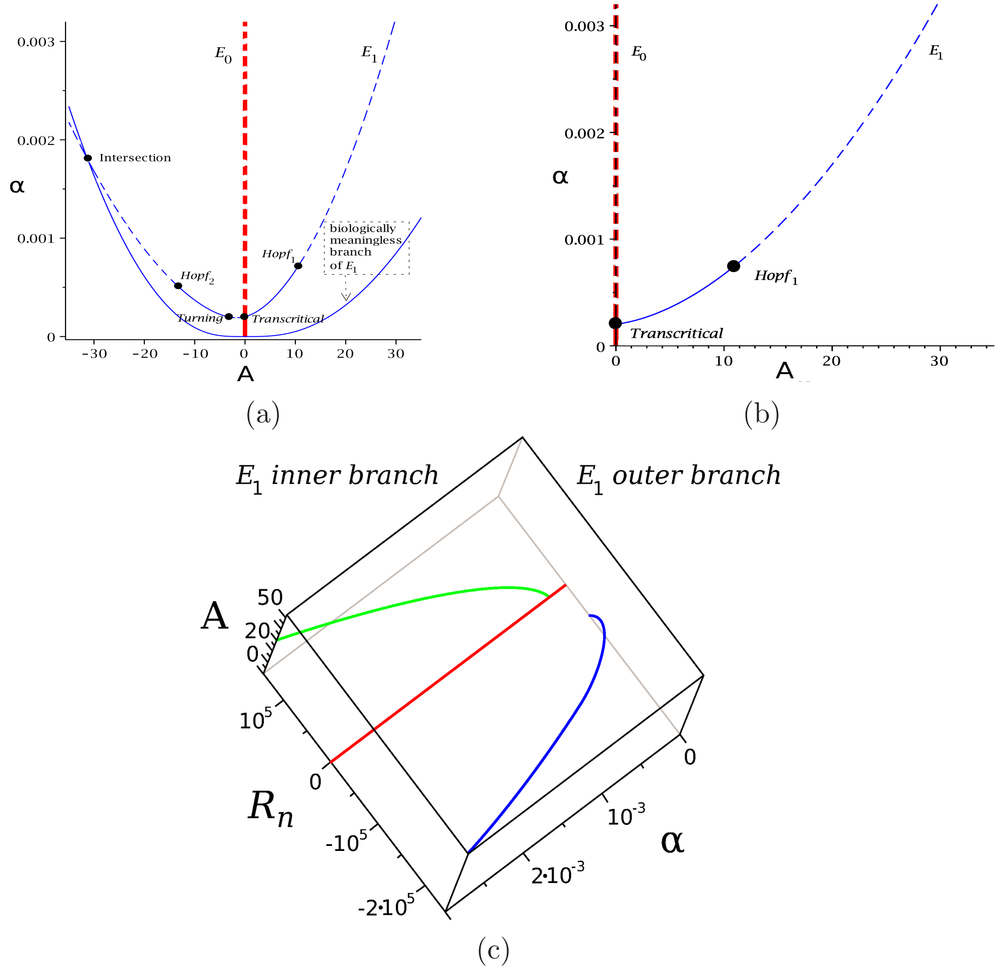

Fig. 1. (a) Complete bifurcation diagram for model (1) projected on the α-A plane, with the red and blue lines denoting E_0 and E_1, respectively; (b) Bifurcation diagram in (a), restricted to the first quadrant; and (c) Bifurcation diagram for model (1) projected on the α-A-R_n space, with the red, green and blue lines denoting E_0, the inner branch of E_1, and the outer branch of E_1 which is biologically meaningless since R_n takes negative values. Here, the dotted and solid lines indicate unstable and stable equilibria, respectively.

$$
\begin{aligned}
a_1(A_1,\alpha) &= \tfrac{1}{40(18A_1^2-9765625\alpha)}(234A_1^2-11250000\alpha A_1-478515625\alpha),\\
a_2(A_1,\alpha) &= \tfrac{1}{5000(18A_1^2-9765625\alpha)^2}[972A_1^5+(1620000000\alpha+20250)A_1^4\\
&\quad +8226562500\alpha A_1^3+(-1856689453125000\alpha^2+268066406250\alpha)A_1^2\\
&\quad -10929107666015625\alpha^2 A_1+4768371582031250000000\alpha^3\\
&\quad -247955322265625000\alpha^2],\\
a_3(A_1,\alpha) &= \tfrac{1}{10000000(18A_1^2-9765625\alpha)^2}[248832A_1^6-1166400A_1^5\\
&\quad -(1307812500000\alpha+72900000)A_1^4+632812500000\alpha A_1^3\\
&\quad +(1296569824218750000\alpha+44494628906250)\alpha A_1^2+5561828613281250000\alpha^2 A_1\\
&\quad -30994415283203125000000\alpha^3+84221363067626953125\alpha^2],\\
a_4(A_1,\alpha) &= \tfrac{1}{50000000(18A_1^2-9765625\alpha)^2}[746496A_1^6-1169437500000\alpha A_1^4+5695312500000\alpha A_1^3\\
&\quad +(733337402343750000\alpha+133483886718750)\alpha A_1^2+3089904785156250000\alpha^2 A_1\\
&\quad -11920928955078125000000\alpha^3+24139881134033203125\alpha^2].
\end{aligned}
$$

Based on the characteristic polynomial (8), we consider possible bifurcations from E_1, including both static bifurcation and dynamic (Hopf) bifurcations. First, the static bifurcation occurs when $P_1(L, A_1, \alpha) = 0$ has zero roots (zero eigenvalues). The simplest case is single zero, i.e., when $a_4(A_1, \alpha) = 0$, and A_1 should simultaneously satisfy $F_1(A_1, \alpha) = 0$ (see equation (7)). Thus, we obtain

$$A_{1s}(\alpha_s) = -\frac{21333593750000000\,\alpha_s^3 + 26617447265625\,\alpha_s^2 - 49464843750\,\alpha_s + 8748000}{3525388312500\,\alpha_s^2 - 4572342000\,\alpha_s + 979776}, \tag{9}$$

where α_s is determined from the equation,

$$F_2(\alpha_s) = \alpha_s\,(13530125\,\alpha_s - 2592)\,(400000\,\alpha_s - 81) = 0. \tag{10}$$

Solving $F_2(\alpha_s) = 0$ for α_s, and then substituting the solutions into $A_{1s}(\alpha_s)$ using Equation (9), yields three critical values. The first one defines a transcritical bifurcation point $(\alpha_t, A_t) = (\frac{81}{400000}, 0) = (0.2025\times 10^{-3}, 0)$, which is exactly the same as that we obtained from the disease-free equilibrium E_0, $\alpha_t = \frac{1}{\lambda_E}(b_1+\mu_A)(b_3+\mu_E) = \frac{1}{1000}(\frac{1}{4}+\frac{1}{5})^2 = \frac{81}{400000}$. Here, the subscript 't' denotes transcritical bifurcation. Moreover, at this critical point, all other Hurwitz arrangements are still positive: $\Delta_1 = \frac{49}{40}$, $\Delta_2 = \frac{5863}{16000}$, and $\Delta_3 = \frac{52767}{6400000}$. This implies that the two equilibrium solutions E_0 and E_1 actually intersect and exchange their stability at this critical point. But it should be noted that the biologically meaninigful equilibrium solution E_1 exists only for $\alpha \geq \alpha_t$ and no further static bifurcation can occur from E_1 for $\alpha > \alpha_t$. The second critical value defines a turning point $(\alpha_{\mathrm{Turning}}, A_{\mathrm{Turning}}) = (\frac{2592}{13530125}, -\frac{1125}{658})$, which has a negative value for A and so is not biologically interesting (see Figure 1(a)). The third critical value is $(\alpha_s, A_{1s}) = (0, 0)$, which is not allowed since α must take positive values for the components $\bar{R}_n$ and $\bar{E}$ in the equilibrium solution E_1 (see Eqns. (6)). Therefore, the equation $F_2(\alpha_s)$ deifnes a unique transcritical bifurcation point.

Now, we turn to consider possible Hopf bifurcations which may occur from the disease equilibrium E_1. To achieve this, we apply Theorem 1 to E_1, where A_1 satisfies the polynomial equation $F_1(A_1, \alpha) = 0$ in (7). Based on the 4th-degree characteristic polynomial $P_1(L, A_1, \alpha)$ (see equation (8)), we apply the formula, $\Delta_3(A_1, \alpha) = a_1a_2a_3 - a_3^2 - a_1^2 a_4$ to solve the two polynomial equations, $\Delta_3(A_1, \alpha) = 0$ and $F_1(A_1, \alpha) = 0$, together with the parameter values given in Table 2.1, yielding two Hopf bifurcation points: $(\alpha_{\mathrm{H1}}, A_{\mathrm{H1}}) \approx (0.7867\times 10^{-3}, 11.4436)$, and $(\alpha_{\mathrm{H2}}, A_{\mathrm{H2}}) \approx (0.5039\times 10^{-3}, -13.1534)$, as shown in Figure 1(a). We only take the biologically meaningful point with two positive entries to get a unique Hopf bifurcation point: $(\alpha_{\mathrm{H}}, A_{\mathrm{H}}) \approx (0.7867\times 10^{-3}, 11.4436)$. Here, the subscript 'H' stands for Hopf bifurcation. At the critical point $(\alpha_{\mathrm{H}}, A_{\mathrm{H}})$, other stability conditions given in Theorem 1 are still satisfied:

$$\begin{aligned} &a_1 \approx 2.098879937, \quad a_2 \approx 0.6310564343, \quad a_3 \approx 0.1144843602, \quad a_4 \approx 0.0314460534, \\ &\Delta_2 \approx 1.2100273294, \quad \Delta_3 \approx -0.1\times 10^{-18} \approx 0. \end{aligned}$$

As a matter of fact, by using these given parameter values, we may numerically compute the Jacobian matrix of system (1) at the equilibrium E_1 to obtain a purely imaginary pair and two negative real eigenvalues: $\pm 0.2335\,i$, -1.7739, and -0.325. Therefore, the disease equilibrium solution E_1 is stable for $\alpha \in (\alpha_t, \alpha_H) \approx (0.2025\times 10^{-3}, 0.7867\times 10^{-3})$ and loses it stabliity at $\alpha = \alpha_H$, a Hopf bifurcation occurs, leading to a family of limit cycles.

In the next section, we will study the Hopf bifurcation from E_1 and use center manifold theory and normal form theory to consider stability and direction of bifurcating limit cycles.

3. Hopf bifurcation and limit cycles: Nonlinear analysis

In this section, we pay attention to the Hopf bifurcation determined in the previous section, and use center manifold theory and normal form theory to find the approximate solutions of the limit cycles and determine their stability. In the following, for convenience, we first briefly describe center manifold theory and normal form theory. Suppose a dynamical system under consideration is described by the following differential equation (D.E.),

$$\dot{\bar{\mathbf{x}}} = \mathbf{F}(\bar{\mathbf{x}}, \bar{\boldsymbol{\mu}}), \quad \bar{\mathbf{x}} \in \mathbf{R}^n, \ \bar{\boldsymbol{\mu}} \in \mathbf{R}^k, \quad \mathbf{F}: \mathbf{R}^{n+k} \to \mathbf{R}^n, \tag{11}$$

where $\bar{\mathbf{x}} = (\bar{x}_1, \bar{x}_2, \ldots, \bar{x}_n)$ is a state vector, $\bar{\boldsymbol{\mu}} = (\bar{\mu}_1, \bar{\mu}_2, \ldots, \bar{\mu}_n)$ is a parameter vector, and the nonlinear vector function $\mathbf{F}$ is assumed to be analytic in $\bar{\mathbf{x}}$ and $\bar{\boldsymbol{\mu}}$. The equilibrium solution $\bar{\mathbf{x}}_e = \bar{\mathbf{x}}_e(\bar{\boldsymbol{\mu}})$ of (11) is determined from $\mathbf{F}(\bar{\mathbf{x}},\, \bar{\boldsymbol{\mu}}) = 0$. We consider Hopf bifurcation, so set $k = 1$ and assume the Jacobian matrix of the system evaluated at the equilibrium solution $\bar{\mathbf{x}}_e$ is given by $J(\mu) = D_{\bar{\mathbf{x}}}\mathbf{F}(\bar{\mathbf{x}}_e,\, \bar{\mu})$, which has a pair of purely imaginary eigenvalues at a critical point $\bar{\mu} = \bar{\mu}_c$, and other eigenvalues have negative real part.

Now, we first apply center manifold theory to reduce the dimension of system (11) and obtain a simplified differential system on the center manifold. Then we apply normal form theory to further simplify the resulting differential system, and perform a bifurcation study of a given type. To achieve this, we introduce a sliding transformation $\bar{\mathbf{x}} = \bar{\mathbf{x}}_e(\bar{\mu}) + \mathbf{u}$, and a parameter shifting $\bar{\mu} = \bar{\mu}_c + \mu$ into system (11) to obtain

$$\dot{\mathbf{u}} = \mathbf{F}\left(\bar{\mathbf{x}}_e(\bar{\mu}_c + \mu) + \mathbf{u},\, \bar{\mu}_c + \mu\right) = \tilde{\mathbf{F}}(\mathbf{u},\, \mu),$$

which yields $D_{\mathbf{u}}\tilde{\mathbf{F}}(\mathbf{0},\, 0) = \tilde{J}$ whose eigenvalues contain an imaginary pair. In addition, introducing another linear transformation $\mathbf{u} = T\mathbf{x}$ such that $J = T^{-1}\tilde{J}T$ is in Jordan canonical form. Therefore, we have obtained the following general D.E.:

$$\dot{\mathbf{x}} = \mathbf{f}(\mathbf{x},\, \mu), \quad \mathbf{x} \in \mathbf{R}^n, \quad \mu \in \mathbf{R}, \quad \mathbf{f}\colon \mathbf{R}^{n+1} \to \mathbf{R}^n, \tag{12}$$

where $\mathbf{f}(\mathbf{x},\, \mu) = T^{-1}\tilde{\mathbf{F}}(T\mathbf{x},\, \mu)$. Now $\mathbf{x} = \mathbf{0}$ is an equilibrium solution of system (12) for any real values of μ, i.e. $\mathbf{f}(\mathbf{0},\, \mu) \equiv \mathbf{0}$ and $J(\mu) = D_{\mathbf{x}}\mathbf{f}(\mathbf{0},\, \mu) = \begin{bmatrix} A(\mu) & 0 \\ 0 & B(\mu) \end{bmatrix}$ with $J(0) = \begin{bmatrix} A(0) & 0 \\ 0 & B(0) \end{bmatrix}$ satisfying $\mathrm{Re}(\lambda(A(0))) = 0,\ \mathrm{Re}(\lambda(B(0))) < 0$. $\lambda(\cdot)$ stands for the eigenvalues of a given matrix. Then, we can rewrite (12) as

$$\begin{aligned} \dot{\mathbf{x}}_c &= A(\mu)\,\mathbf{x}_c + \mathbf{f}_c(\mathbf{x}_c,\, \mathbf{x}_s;\, \mu), \\ \dot{\mathbf{x}}_s &= B(\mu)\,\mathbf{x}_s + \mathbf{f}_s(\mathbf{x}_c,\, \mathbf{x}_s;\, \mu), \end{aligned} \tag{13}$$

where $\mathbf{x} = (\mathbf{x}_c, \mathbf{x}_s)^T$, $\mathbf{x}_c$ and $\mathbf{x}_s$ are state variables associated with the eigenvalues of the linearized systems with zero and negative real part, respectively. $n_c + n_s = n$ (for Hopf bifurcation, $n_c = 2$), and

$$A(\mu) = A + \bar{A}\,\mu, \quad B(\mu) = B + \bar{B}\,\mu. \tag{14}$$

Moreover, $\mathbf{f}_c$ and $\mathbf{f}_s$ satisfy $\mathbf{f}_c(\mathbf{0},\, \mathbf{0};\, 0) = \mathbf{f}_s(\mathbf{0},\, \mathbf{0};\, 0) = 0$ and $\frac{\partial \mathbf{f}_c(\mathbf{0},\mathbf{0};0)}{\partial \mathbf{x}_c} = \frac{\partial \mathbf{f}_c(\mathbf{0},\mathbf{0};0)}{\partial \mathbf{x}_s} = \frac{\partial \mathbf{f}_c(\mathbf{0},\mathbf{0};0)}{\partial \mu} = \frac{\partial \mathbf{f}_s(\mathbf{0},\mathbf{0};0)}{\partial \mathbf{x}_c} = \frac{\partial \mathbf{f}_s(\mathbf{0},\mathbf{0};0)}{\partial \mathbf{x}_s} = \frac{\partial \mathbf{f}_s(\mathbf{0},\mathbf{0};0)}{\partial \mu} = 0$. By center manifold theory, there exists an analytic function $\mathbf{h}$, such that $\mathbf{x}_s = \mathbf{h}(\mathbf{x}_c;\, \mu)$ with $\mathbf{h}(\mathbf{0};\, 0) = D\mathbf{h}(\mathbf{0};\, 0) = \mathbf{0}$. Thus, $\dot{\mathbf{x}}_s = D\mathbf{h}(\mathbf{x}_c;\, \mu)\,\dot{\mathbf{x}}_c$, which can be rewritten as

$$\mathcal{N}(\mathbf{h}(\mathbf{x}_c;\, \mu)) \equiv D\mathbf{h}(\mathbf{x}_c;\, \mu)\big[A(\mu)\mathbf{x}_c + \mathbf{f}_c(\mathbf{x}_c,\, \mathbf{h}(\mathbf{x}_c;\, \mu);\, \mu)\big] - B(\mu)\mathbf{h}(\mathbf{x}_c;\, \mu) - \mathbf{f}_s(\mathbf{x}_c,\, \mathbf{h}(\mathbf{x}_c;\, \mu)) = 0. \tag{15}$$

In general, the above equation with the boundary conditions $\mathbf{h}(\mathbf{0};\, 0) = D\mathbf{h}(\mathbf{0};\, 0) = \mathbf{0}$ can not be solved analytically. To find the approximation of $\mathbf{h}(\mathbf{x}_c;\, \mu)$, we use the Taylor series of $\mathbf{h}(\mathbf{x}_c;\, \mu)$ expanded near $(\mathbf{x}_c;\, \mu) = (\mathbf{0};\, 0)$ with undetermined coefficients, and then expanding (15) and balancing the coefficients of like powers to determine the coefficients in $\mathbf{h}(\mathbf{x}_c;\, \mu)$, and so an approximation of $\mathbf{x}_s = \mathbf{h}(\mathbf{x}_c;\, \mu)$ is obtained.

We now consider the projection of the vector field on the center manifold $W^c = \{(\mathbf{x}_c,\, \mathbf{x}_s) | \mathbf{x}_s = \mathbf{h}(\mathbf{x}_c;\, \mu)\}$, yielding $\dot{\mathbf{x}}_c = A(\mu)\,\mathbf{x}_c + \mathbf{f}_c(\mathbf{x}_c,\, \mathbf{h}(\mathbf{x}_c;\, \mu);\, \mu)$ or

$$\dot{\mathbf{x}}_c = A(\mu)\,\mathbf{x}_c + \mathbf{f}_c(\mathbf{x}_c;\, \mu), \quad \mathbf{x}_c \in \mathbf{R}^2,\ \mu \in \mathbf{R}, \tag{16}$$

satisfying $\mathbf{f}_c(\mathbf{0};\, 0) = D\mathbf{f}_c(\mathbf{0};\, 0) = 0$, and $A(\mu) = A + \bar{A}\,\mu$ where $A = \begin{bmatrix} 0 & \omega \\ -\omega & 0 \end{bmatrix}$ and $\bar{A} = \begin{bmatrix} a_{11} & a_{12} \\ a_{21} & a_{22} \end{bmatrix}$. Now applying the method of normal forms to system (16) and put the result in the polar coordinates yields

$$\begin{aligned} \dot{r} &= r\,(\upsilon_0\mu + \upsilon_1 r^2 + \upsilon_2 r^4 + \ldots), \\ \dot{\theta} &= \omega + \tau_0\mu + \tau_1 r^2 + \tau_2 r^4 + \ldots, \end{aligned} \tag{17}$$

where r and θ denote the amplitude and phase of motion, respectively; υ_0 and τ_0 can be obtained from linear analysis, while $\upsilon_1,\, \upsilon_2, \ldots$ and $\tau_1,\, \tau_2, \ldots$ are obtained from nonlinear analysis. We have the following theorem for finding υ_0 and τ_0.

Theorem 2. *For the linearized system of (16),*

$$\dot{\mathbf{x}}_c = A(\mu)\,\mathbf{x}_c = \begin{bmatrix} a_{11}\,\mu & \omega + a_{12}\,\mu \\ -\omega + a_{21}\,\mu & a_{22}\,\mu \end{bmatrix} \mathbf{x}_c,$$

the following is true,

$$\upsilon_0 = \frac{1}{2}(a_{11} + a_{22}), \quad \tau_0 = \frac{1}{2}(a_{12} - a_{21}). \tag{18}$$

Proof. This is a 2-dimensional system. Let $\mathbf{x}_c = (x_{c_1}, x_{c_2})^T$. There exits an invertible matrix T, given by

$$P = \begin{bmatrix} -(\omega + a_{12}\,\mu) & 0 \\ \frac{1}{2}(a_{11} - a_{22})\,\mu & -\omega\sqrt{1 + \frac{1}{\omega}(a_{12} - a_{21})\,\mu + \frac{1}{\omega^2}\left[a_{12}a_{21} - \frac{1}{4}(a_{11} - a_{22})^2\right]\mu^2} \end{bmatrix}, \tag{19}$$

which is used in the transformation $(x_{c_1}, x_{c_2})^T = P\,(y_1, y_2)^T$ to yield

$$\begin{pmatrix} \dot{y}_1 \\ \dot{y}_2 \end{pmatrix} = P^{-1}\,A\,P \begin{pmatrix} y_1 \\ y_2 \end{pmatrix} = \begin{bmatrix} \frac{1}{2}(a_{11} + a_{22})\,\mu & \bar{\omega} \\ -\bar{\omega} & \frac{1}{2}(a_{11} + a_{22})\,\mu \end{bmatrix} \begin{pmatrix} y_1 \\ y_2 \end{pmatrix}, \tag{20}$$

where P^{-1} is the inverse matrix of P, and

$$\bar{\omega} = \omega\sqrt{1 + \tfrac{1}{\omega}(a_{12} - a_{21})\,\mu + \tfrac{1}{\omega^2}\left[a_{12}a_{21} - \tfrac{1}{4}(a_{11} - a_{22})^2\right]\mu^2}.$$

Next, we put the new system (20) in polar coordinates, via $y_1 = r\,\sin\theta$, $y_2 = r\,\cos\theta$. Thus, $r^2 = y_1^2 + y_2^2$, and $\tan\theta = \frac{y_1}{y_2}$. Therefore, $2\,r\,\dot{r} = 2\,y_1\,\dot{y}_1 + 2\,y_2\,\dot{y}_2$, yielding

$$\dot{r} = \frac{1}{2}(a_{11} + a_{22})\,\mu\,r = \upsilon_0\,\mu\,r. \tag{21}$$

and $\sec^2\theta\,\dot{\theta} = \frac{\dot{x}_1\,x_2 - \dot{x}_2\,x_1}{x_2^2}$, giving

$$\begin{aligned} \dot{\theta} &= \frac{\dot{x}_1\,x_2 - \dot{x}_2\,x_1}{(1 + x_1^2/x_2^2)\,x_2^2} = \omega\sqrt{1 + \tfrac{1}{\omega}(a_{12} - a_{21})\,\mu + \tfrac{1}{\omega^2}\left[a_{12}a_{21} - \tfrac{1}{4}(a_{11} - a_{22})^2\right]\mu^2} \\ &= \omega\left[1 + \tfrac{1}{2\omega}(a_{12} - a_{21})\,\mu\right] + O(\mu^2) \\ &= \omega + \tfrac{1}{2}(a_{12} - a_{21})\,\mu + O(\mu^2) \\ &= \omega + \tau_0\,\mu + O(\mu^2). \end{aligned} \tag{22}$$

The proof of Theorem 2 is complete. ■

Note that if the original system is a nonlinear system, given in the general form, $\dot{\mathbf{x}}_c = \mathbf{f}(\mathbf{x}_c, \mu)$, with $\mathbf{f}(\mathbf{0}, 0) = 0$, and $J(\mathbf{0}, 0) = D_{\mathbf{x}_c}\mathbf{f}(\mathbf{0}, 0) = \begin{bmatrix} 0 & \omega \\ -\omega & 0 \end{bmatrix}$. Then $a_{ij} = \frac{\partial f_i^2}{\partial x_j\,\partial\mu}$, $i, j = 1, 2$.

Finally, to find $\upsilon_1, \upsilon_2, \ldots$ and $\tau_1, \tau_2, \ldots$, we set $\mu = \mu_c = 0$ in system (16) to consider

$$\dot{\mathbf{x}}_c = A(0)\,\mathbf{x}_c + \mathbf{f}_c(\mathbf{x}_c, \mathbf{h}(\mathbf{x}_c; 0); 0) = A\,\mathbf{x}_c + \mathbf{f}_c(\mathbf{x}_c),$$

and apply normal form theory (e.g., see [Guckenheimer & Holmes, 1990]) to obtain

$$\begin{aligned} \dot{x}_{c_1} = {} & x_{c_1}[\upsilon_1\,(x_{c_1}^2 + x_{c_2}^2) + \upsilon_2\,(x_{c_1}^2 + x_{c_2}^2)^2 + \ldots] \\ & + x_{c_2}[\omega + \tau_1\,(x_{c_1}^2 + x_{c_2}^2) + \tau_2\,(x_{c_1}^2 + x_{c_2}^2)^2 + \ldots], \\ \dot{x}_{c_2} = {} & -x_{c_1}[\omega + \tau_1\,(x_{c_1}^2 + x_{c_2}^2) + \tau_2\,(x_{c_1}^2 + x_{c_2}^2)^2 + \ldots] \\ & + x_{c_2}[\upsilon_1\,(x_{c_1}^2 + x_{c_2}^2) + \upsilon_2\,(x_{c_1}^2 + x_{c_2}^2)^2 + \ldots], \end{aligned}$$

which can be written via $x_{c_1} = r\sin\theta$, $x_{c_2} = r\cos\theta$ as

$$\begin{aligned} \dot{r} &= r\,(\upsilon_1 r^2 + \upsilon_2 r^4 + \ldots), \\ \dot{\theta} &= \omega + \tau_1 r^2 + \tau_2 r^4 + \ldots, \end{aligned}$$

The proof can be found in [Yu, 1998].

It should be pointed out that the above two steps in computing the normal form of genral nonlienar systems can be combined into one procedure, e.g., see [Yu, 1998, 2003].

3.1. *Normal form computation associated with the Hopf bifurcation from* $\mathbf{E_1}$

Now we apply normal form theory and the Maple program developed in [Yu, 1998] to system (1) to analyze the Hopf bifurcation which occurs at the critical point $(\alpha_{\mathrm{H}}, A_{\mathrm{H}}) \approx (7.8666 \times 10^{-4}, 11.4436)$ (with other parameters given in Table 2.1). We show how to find the normal form for system (1) associated with this Hopf critical point.

Let $\alpha = \alpha_H + \mu$, where μ is a small perturbation (bifurcation) parameter. Then, with

$$P = \begin{bmatrix} -0.0001169099 & -0.0002184341 & -0.0008788039 & -0.0001219983 \\ -0.8049052552 & 0.0 & 0.1059811404 & 0.5249612314 \\ -0.3405368387 & 0.3976613541 & -0.0134675000 & -0.8399379702 \\ -0.1318126011 & -0.2462783299 & 0.9942765471 & -0.1375496158 \end{bmatrix}$$

we introduce the affine transformation

$$\begin{pmatrix} A \\ R_n \\ R_d \\ E \end{pmatrix} = \begin{pmatrix} \bar{A}(\mu) \\ \bar{R}_n(\bar{A}(\mu), \mu) \\ \bar{R}_d(\bar{A}(\mu), \mu) \\ \bar{E}(\bar{A}(\mu), \mu) \end{pmatrix} + P \begin{pmatrix} x_1 \\ x_2 \\ x_3 \\ x_4 \end{pmatrix}, \tag{23}$$

where

$$\begin{aligned} \bar{R}_n(\bar{A}(\mu), \mu) &= \frac{-0.002304\,(\bar{A} + 13.65733522 + 17361.11111\,\mu)\,\bar{A}}{0.4608 \times 10^{-7}\,\bar{A}^2 - .1966656271 \times 10^{-4} - 0.025\,\mu}, \\ \bar{R}_d(\bar{A}(\mu), \mu) &= \frac{-0.002304\,(\bar{A} + 13.65733522 + 17361.11111\,\mu)\,\bar{A}}{0.4608 \times 10^{-7}\,\bar{A}^2 - 0.1966656271 \times 10^{-4} - 0.025\,\mu}, \\ \bar{E}(\bar{A}(\mu), \mu) &= \frac{-7812.5\,(0.02458320339 + 0.7866625085 \times 10^{-3}\,\bar{A} + \bar{A}\,\mu + 31.25\,\mu)\,\bar{A}}{(0.0007866625084 + \mu)\,(\bar{A}^2 - 426.7917255 - 542534.7222\,\mu)}, \end{aligned}$$

while $\bar{A}$ and μ have the following relation:

$$\begin{aligned} F_{4a} &= 0.21233664 \times 10^{-11}\,\bar{A}^4 + (-0.191442188 \times 10^{-8} - 0.24336 \times 10^{-5}\,\mu)\,\bar{A}^2 \\ &\quad - (0.6371966318 \times 10^{-8} + 0.81 \times 10^{-5}\,\mu)\,\bar{A} - 0.9956197372 \times 10^{-7} \\ &\quad - 0.1265625 \times 10^{-3}\,\mu + 0.625\,(0.7866625084 \times 10^{-3} + \mu)^2 \\ &= 0, \end{aligned}$$

into system (1) to obtain

$$\dot{x}_i = F_i(x_1, x_2, x_3, x_4; \mu), \quad i = 1, 2, 3, 4, \tag{24}$$

in which

$$\begin{aligned} F_1 &= 0.2335496834\,x_2 + 0.1 \times 10^{-5} \\ &\quad +(79.07737301\,x_1 + 65.85310456\,x_2 - 917.0159663\,x_3 + 73.44534378\,x_4)\,\mu + o(\mu) \\ &\quad +0.6907346099 \times 10^{-7}\,x_1^2 - 0.7871759754 \times 10^{-6}\,x_1\,x_2 + 0.3970174728 \times 10^{-6}\,x_1\,x_3 \\ &\quad +0.283435609 \times 10^{-7}\,x_1\,x_4 - 0.2450834082 \times 10^{-6}\,x_3\,x_2 + 0.2071989330 \times 10^{-4}\,x_3^2 \\ &\quad +0.3049539696 \times 10^{-6}\,x_3\,x_4 - 0.1037827494 \times 10^{-5}\,x_4\,x_2 - 0.456398326 \times 10^{-7}\,x_4^2 \\ &\quad -0.1711886771 \times 10^{-5}\,x_2^2, \end{aligned}$$

$$
\begin{aligned}
F_2 = &-0.2335496834\, x_1 + 0.3 \times 10^{-5} \\
&+(600.2222024\, x_1 + 735.9644840\, x_2 - 1588.592053\, x_3 + 583.6348214\, x_4)\, \mu + o(\mu) \\
&+0.1870133257 \times 10^{-5}\, x_1^2 + 0.2707944533 \times 10^{-5}\, x_1\, x_2 - 0.165759520 \times 10^{-6}\, x_1\, x_3 \\
&+0.3428802216 \times 10^{-5}\, x_1\, x_4 - 0.1445942971 \times 10^{-6}\, x_3\, x_2 - 0.5061600581 \times 10^{-5}\, x_3^2 \\
&-0.154680119 \times 10^{-6}\, x_3\, x_4 + 0.1939706942 \times 10^{-5}\, x_4\, x_2 + 0.1541570112 \times 10^{-5}\, x_4^2 \\
&-0.1468948484 \times 10^{-5}\, x_2^2, \\
F_3 = &-1.773879937\, x_3 - 0.2 \times 10^{-5} \\
&+(21.72751810\, x_1 + 168.3180208\, x_2 - 62.7868030\, x_3 + 36.82458413\, x_4)\, \mu + o(\mu) \\
&+0.3 \times 10^{-15}\, x_1^2 - 0.5 \times 10^{-16}\, x_1\, x_2 + 0.4457936798 \times 10^{-5}\, x_1\, x_3 \\
&+0.4 \times 10^{-15}\, x_1\, x_4 - 0.2385968125 \times 10^{-5}\, x_3\, x_2 - 0.2371384210 \times 10^{-6}\, x_3^2 \\
&+0.3464744128 \times 10^{-5}\, x_3\, x_4 - 0.1 \times 10^{-15}\, x_4\, x_2 + 0.2 \times 10^{-15}\, x_4^2, \\
F_4 = &-0.3250000000\, x_4 + .1 \times 10^{-5} \\
&+(251.7612101\, x_1 + 319.0383240\, x_2 - 379.3117812\, x_3 + 245.9493920\, x_4)\, \mu + o(\mu) \\
&+0.8573938681 \times 10^{-6}\, x_1^2 + 0.1601198369 \times 10^{-5}\, x_1\, x_2 - 0.310918787 \times 10^{-6}\, x_1\, x_3 \\
&+0.1611845343 \times 10^{-5}\, x_1\, x_4 + 0.6916390751 \times 10^{-7}\, x_3\, x_2 - 0.1079305444 \times 10^{-4}\, x_3^2 \\
&-0.2524231766 \times 10^{-6}\, x_3\, x_4 + 0.1339104819 \times 10^{-5}\, x_4\, x_2 + 0.7483468117 \times 10^{-6}\, x_4^2 \\
&-0.14090733 \times 10^{-8}\, x_2^2,
\end{aligned}
$$

where $o(\mu)$ represents higher-order terms of μ. Now, the Jacobian of system (24) evaluated on the equilibrium, $x_i = 0$, $i = 1, 2, 3, 4$, at the critical point, $\mu = 0$ (corresponding to the disease equilibrium for model (1)) is in the Jordan canonical form:

$$
J = \begin{bmatrix} 0 & 0.233549683 & 0 & 0 \\ -0.233549683 & 0 & 0 & 0 \\ 0 & 0 & -1.773879938 & 0 \\ 0 & 0 & 0 & -0.3250000000 \end{bmatrix}
$$

Applying the formula (18) to system (24), we obtain

$$
\begin{aligned}
\upsilon_0 &= \frac{1}{2}\left(\frac{\partial^2 F_1}{\partial x_1\, \partial \mu} + \frac{\partial^2 F_2}{\partial x_2\, \partial \mu}\right)\bigg|_{x_i=0,\, \mu=0} = 34.2047656142, \\
\tau_0 &= \frac{1}{2}\left(\frac{\partial^2 F_1}{\partial x_2\, \partial \mu} - \frac{\partial^2 F_2}{\partial x_1\, \partial \mu}\right)\bigg|_{x_i=0,\, \mu=0} = 132.8997934535.
\end{aligned} \tag{25}
$$

Next, substituting $\mu = 0$ into (24) and then applying the Maple program [Yu, 1998] yields

$$
\upsilon_1 = -0.2016072570 \times 10^{-11}, \quad \tau_1 = -0.1318624299 \times 10^{-10}. \tag{26}
$$

Therefore, the normal form associated with this Hopf bifurcation, up to third order terms, is given by

$$
\begin{aligned}
\dot{r} &= r\,(34.2047656142\, \mu - 0.2016072570 \times 10^{-11}\, r^2), \\
\dot{\theta} &= 0.233549683 + 132.8997934535\, \mu - 0.1318624299 \times 10^{-10}\, r^2.
\end{aligned} \tag{27}
$$

The steady-state solutions of equation (27) are determined by $\dot{r} = \dot{\theta} = 0$, resulting in

$$
\bar{r} = 0, \quad \bar{r}^2 \approx 0.1696603893 \times 10^{14}\, \mu. \tag{28}
$$

The equilibrium solution $\bar{r} = 0$ represents the disease equilibrium E_1 of model (1). A linear analysis on the first differential equation of (27) shows that $\frac{d}{dr}\left(\frac{dr}{dt}\right)\big|_{\bar{r}=0} = \upsilon_0\, \mu$, and thus $\bar{r} = 0$ (E_1) is stable (unstable) for $\mu < 0$ (> 0), as expected. When μ is increased from negative to cross zero, a Hopf bifurcation occurs and the amplitude of the bifurcating limit cycles is approximated by the non-zero steady state solution,

$$
\bar{r} \approx 0.4118985182 \times 10^7 \sqrt{\mu} \quad (\mu > 0). \tag{29}
$$

Since $\frac{\mathrm{d}}{\mathrm{d}r}\left(\frac{\mathrm{d}r}{\mathrm{d}t}\right)\big|_{(29)} = 2v_1\mu < 0$ $(\mu > 0, v_1 < 0)$, it indicates that the Hopf bifurcation is supercritical since $v_1 < 0$ and so the bifurcating limit cycles are stable. The equation (29) gives the approximate amplitude of the bifurcating limit cycles, while the phase of the motion is determined by $\theta = \omega\, t$, where ω is given by

$$\omega = \frac{\mathrm{d}\theta}{\mathrm{d}t}\bigg|_{(29)} = 0.233549683 - 90.8185182\,\mu. \tag{30}$$

Having found the non-zero steady-state solution (limit cycle) in terms of $\bar{r}$ and $\theta = \omega\, t$, the periodic solution of equation (24) can be written in a general form:

$$\begin{aligned} x_1(\mu) &= \bar{r}\,\cos(\omega\, t) + h_1(\bar{r}\,\cos(\omega\, t),\, \bar{r}\,\sin(\omega\, t)),\\ x_2(\mu) &= -\bar{r}\,\sin(\omega\, t) + h_2(\bar{r}\,\cos(\omega\, t),\, \bar{r}\,\sin(\omega\, t)),\\ x_i(\mu) &= h_i(\bar{r}\,\cos(\omega\, t),\, \bar{r}\,\sin(\omega\, t)), \quad i = 3,4,\ h_i \text{ starts from second-order term,} \end{aligned} \tag{31}$$

while the first-order approximation of the limit cycles is given by

$$x_1(\mu) = \bar{r}\,\cos(\omega\, t), \quad x_2(\mu) = -\bar{r}\,\sin(\omega\, t), \quad x_3 = x_4 = 0,$$

where $\bar{r}$ and ω are given in equations (29) and (30), respectively. However, in order to get higher-order (e.g., third order) approximate solutions of the oscillation in terms of the original variables A, R_n, R_d, and E for a comparison with the numerical simulation to be discussed in the next section, we need the nonlinear transformations (including the center manifold transformation and the normal form transformation) between x_i, $(i = 1,2,3,4)$ and the polar coordinates $(r,\, \theta)$. Fortunately, these nonlinear transformations can be obtained directly from the computer output of the Maple program [Yu, 1998] as follows:

$$\begin{aligned} x_1(t) =\ & \cos(\omega\, t)\,\bar{r} + \big[0.8588852860\times10^{-6} - 0.3506344360\times10^{-5}\,\cos(2\,\omega\, t)\\ & + 0.4474326340\times10^{-5}\,\sin(2\,\omega\, t)\big]\,\bar{r}^2\\ & + \big[0.1097332343\times10^{-10}\cos(3\omega t) + 0.3484198508\times10^{-10}\sin(3\omega t)\big]\,\bar{r}^3,\\ x_2(t) =\ & -\sin(\omega\, t)\,\bar{r} + \big[0.3517053177\times10^{-5} + 0.5135844613\times10^{-5}\cos(2\omega t)\\ & + 0.5327445638\times10^{-5}\sin(2\omega t)\big]\,\bar{r}^2\\ & - \big[0.3403071221\times10^{-10}\cos(\omega t) + 0.4194098549\times10^{-11}\sin(\omega t)\\ & + 0.4874935933\times10^{-10}\cos(3\omega t) - 0.532632423\times10^{-11}\sin(3\omega t)\big]\,\bar{r}^3,\\ x_3(t) =\ & \big[0.8456040162\times10^{-16} + 0.7213644930\times10^{-16}\,\cos(2\,\omega\, t)\\ & + 0.4718182329\times10^{-16}\,\sin(2\,\omega\, t)\big]\,\bar{r}^2,\\ x_4(t) =\ & \big[0.1316899684\times10^{-5} - 0.1841270059\times10^{-6}\,\sin(2\,\omega\, t)\\ & + 0.1585867935\times10^{-5}\,\cos(2\,\omega\, t)\big]\,\bar{r}^2\\ & + \big[0.1207672844\times10^{-10}\,\cos(\omega\, t) + 0.1812966212\times10^{-10}\,\sin(\omega\, t)\\ & - 0.8220638067\times10^{-11}\cos(3\omega t) + 0.1214100228\times10^{-10}\sin(3\omega t)\big]\,\bar{r}^3. \end{aligned} \tag{32}$$

Finally, with the above transformations we can now use the affine transformation (23) to obtain the periodic solution in terms of the original variables.

4. Generalized Hopf Bifurcation Leading to Multiple Limit Cycles

In previous sections, we have given a detailed analysis on Hopf bifurcation, which is limited to bifurcation of single limit cycle. However, disease models may exhibit complex dynamical behaviours caused by bifurcation of multiple limit cycles, yielding bistable or multiple stable solutions involving equilibria and steady motions. It has been noted that such a study is often ignored in the literature on the analysis of practical systems, in particular, on biological systems, since the analysis is not easy even for 2-dimensional systems. Almost all published works are limited to bifurcation of single limit cycle with very few of them using numerical simulation to show two limit cycles.

In this section, we will use the reduced 3-dimensional model presented in [Zhang *et al.*, 2014] to prove the existence of two limit cycles bifurcating from a degenerate Hopf critical point. To reduce the 4-dimensional system (1) to a 3-dimensional model, we assume the following:

(1) Only the suppression for which Treg (R_n and R_d) acts on pAPC (A), not on effector T cells (E), is considered, resulting in $\sigma_3 = 0$.
(2) Except for E, the IL-2 sources are not considered, yielding $\beta = 0$.
(3) Quasi-steady state assumption is applied to the last equation of model (1), leading to $\dot{E} \approx 0$, and thus the state variable E can be eliminated from the system.

Under the above assumptions, system (1) becomes

$$\begin{aligned} \dot{A} &= \frac{\alpha\lambda_E}{b_3+\mu_A}\, A - \sigma_1(R_n + dR_d)A - (b_1+\mu_A)A, \\ \dot{R}_n &= \frac{\pi_3\lambda_E}{b_1+\mu_A}\, A^2 - (\mu_n+\xi)R_n, \\ \dot{R}_d &= c\,\xi R_n - \mu_d R_d. \end{aligned} \tag{33}$$

To further simplify the analysis, introducing the following dimensionless transformation,

$$A = \mu_1 X, \quad R_n = \mu_2 Y, \quad R_d = \mu_3 Z, \quad \tau = \mu_4 t, \tag{34}$$

where

$$\mu_1 = \mu_d \sqrt{\tfrac{b_3+\mu_e}{\sigma_1\pi_3\lambda_E}}, \quad \mu_2 = \frac{\mu_d}{\sigma_1}, \quad \mu_3 = \frac{c\,\xi}{\sigma_1}, \quad \mu_4 = \mu_d,$$

into (48) we obtain

$$\begin{aligned} \frac{dX}{d\tau} &= \big(m_1 - m_2 - Y - DZ\big)\, X, \\ \frac{dY}{d\tau} &= X^2 - m_3\, Y, \\ \frac{dZ}{d\tau} &= Y - Z, \end{aligned} \tag{35}$$

where the new parameters are given by

$$m_1 = \frac{\alpha\,\lambda_E}{\mu_d(b_3+\mu_E)}, \quad m_2 = \frac{b_1+\mu_A}{\mu_d}, \quad m_3 = \frac{\mu_n+\xi}{\mu_d}, \quad D = \frac{d\,c\,\xi}{\mu_d}.$$

Here, note that only m_1 contains α which is usually treated as a bifurcation parameter. Using the parameter values given in Table 2.1 we have

$$\mu_1 = \frac{25\sqrt{6}}{4}\,[A], \quad \mu_2 = \frac{2\times 10^5}{3}\,[R_n]. \quad \mu_3 = \frac{2\times 10^5}{3}\,[R_d], \quad \mu_4 = \frac{1}{5}/\text{day},$$

which agree with the units of the state variables and time. Moreover, assuming $\alpha = \frac{1}{2000} = 0.0005$, we have the new parameters which are indeed dimensionless, given by

$$m_1 = \frac{50}{9} \approx 5.555556, \quad m_2 = \frac{9}{4} = 2.25, \quad m_3 = \frac{5}{8} = 0.625, \quad D = 2. \tag{36}$$

It is easy to obtain two equilibrium solutions from (35) as follows:

$$\mathrm{E}_0 : (0,0,0), \quad \mathrm{E}_1 : \Big(\sqrt{\tfrac{m_3(m_1-m_2)}{1+D}},\ \tfrac{m_1-m_2}{1+D},\ \tfrac{m_1-m_2}{1+D}\Big), \ (m_1 \ge m_2). \tag{37}$$

A simple linear analysis based on the Jacobian of (35) shows that when $m_1 < m_2$, the disease-free equilibrium E_0 is stable while the disease equilibrium E_1 does not exist; when $m_1 > m_2$, E_0 becomes unstable and E_1 emerges. The characteristic polynomial for E_1 is given by

$$P_1(\lambda) = \lambda^3 + (m_3+1)\,\lambda^2 + \tfrac{m_3[1+D+2(m_1-m_2)]}{1+D}\,\lambda + 2m_3(m_1-m_2), \tag{38}$$

indicating that $m_1 = m_2$ defines a transcritical bifurcation point between E_0 and E_1, and there is no static bifurcation from E_1 when $m_1 > m_2$. Therefore, the only possible bifurcation from E_1 is Hopf bifurcation. The critical Hopf bifurcation point is determined by the condition, $\Delta_2 = 0$, where

$$\begin{aligned}\Delta_2 &= (1+m_3)\tfrac{m_3\left[1+D+2(m_1-m_2)\right]}{1+D} - 2m_3(m_1-m_2)\\ &= \tfrac{m_3}{1+D}\left\{2m_3(m_1-m_2)+(1+m_3)-\left[2\,(m_1-m_2)-(1+m_3)\right]D\right\}.\end{aligned}$$

It is easy to see that when $m_1 > m_2$ and $2\,(m_1 - m_2) - (1 + m_3) < 0$, E_1 is always stable, and a Hopf bifurcation occurs from E_1 only if $2\,(m_1 - m_2) - (1 + m_3) > 0$. Hence, the Hopf critical point is defined by

$$D_{\rm H} = \frac{2m_3(m_1-m_2)+(1+m_3)}{2(m_1-m_2)-(1+m_3)}, \quad \big(2\,(m_1-m_2)-(1+m_3)>0,\ m_1>m_2\big), \tag{39}$$

where the subcritical H denotes Hopf bifurcation. Further, suppose the characteristic polynomial equation $P_1(\lambda) = 0$ has one real eigenvalue $\lambda_1(D)$ and a complex conjugate, $\lambda_{2,3}(D) = \alpha(D) \pm i\,\omega(D)$. It should be noted that $\lambda(D)$, $\alpha(D)$ and $\omega(D)$ contain other parameters, m_1, m_2 and m_3. Then, at this critical point $D = D_{\rm H}$, we have

$$\lambda_1(D_{\rm H}) = -\,(1+m_3) < 0, \quad \alpha(D_{\rm H}) = 0, \quad \text{and} \quad \omega(D_{\rm H}) = \omega_c = \sqrt{\tfrac{2m_3(m_1-m_2)}{1+m_3}} > 0, \quad (m_1{>}m_2).$$

Moreover, we can show that the transversal condition is satisfied:

$$\frac{\partial\,\alpha}{\partial\,D}(D_{\rm H}) = \frac{m_3\left[2(m_1-m_2)-(1+m_3)\right]^2}{4(m_1-m_2)\left[(1+m_3)^3+2m_3(m_1-m_2)\right]} > 0.$$

Next, introducing the following affine transformation

$$\begin{pmatrix} X\\ Y\\ Z\end{pmatrix} = \begin{pmatrix}\sqrt{\frac{m_3(m_1-m_2)}{1+D}}\\ \frac{m_1-m_2}{1+D}\\ \frac{m_1-m_2}{1+D}\end{pmatrix} + P\begin{pmatrix}x_1\\ x_2\\ x_3\end{pmatrix}, \tag{40}$$

where

$$P = \begin{bmatrix} -\sqrt{\frac{m_3[2(m_1-m_2)-(1+m_3)]}{2(1+m3)}} & \frac{(1+m_3)^{3/2}\omega_c}{m_3\sqrt{2m_3[2(m_1-m_2)-(1+m_3)]}} & \frac{m_3(1+m_3)}{\sqrt{2[2(m_1-m_2)-(1+m_3)]}}\\ 1 & \omega_c & -m_3\\ 1 & 0 & 1\end{bmatrix},$$

into system (35) we obtain

$$\begin{aligned}\frac{dx_1}{d\tau} &= \omega_c\,x_2 + \frac{1}{2C_1C_3}\Big[m_3(1+m_3)C_2C_3x_1^2 + 2(1+m_3)(m_1-m_2)C_4x_2^2\\ &\quad +3m_3(1+m_3)^3x_3^2 + 2\omega_cC_5x_1x_2 - 4m_3(1+m_3)^2(m_1-m_2-1-m_3)x_1x_3\\ &\quad +2(1+m_3)\omega_cC_6x_2x_3\Big],\\ \frac{dx_2}{d\tau} &= -\,\omega_c\,x_1 + \frac{1}{2C_1C_3}\Big[\omega_cC_3C_6x_1^2 - 2(1+m_3)^3(m_1-m_2-1-m_3)\omega_cx_2^2\\ &\quad +\tfrac{(1+m_3)^2\omega_c}{m_1-m_2}C_7x_3^2 - (1+m_3)^2C_8x_1x_2 - \tfrac{(1+m_3)\omega_c}{m_1-m_2}C_9x_1x_3\\ &\quad -2(1+m_3)^2(1+m_3^3)x_2x_3\Big],\\ \frac{dx_3}{d\tau} &= -\,(1+m_3)x_3 + \frac{1}{2C_1C_3}\Big[m_3(1+m_3)C_2C_3x_1^2 - 2(1+m_3)(m_1-m_2)C_4x_2^2\\ &\quad -3(1+m_3)^3m_3x_3^2 - 2\omega_cC_{10}x_1x_2 + 4m_3(1+m_3)^2(m_1-m_2-1-m_3)x_1x_3\\ &\quad -2(1+m_3)\omega_cC_6x_2x_3\Big],\end{aligned} \tag{41}$$

where

$$
\begin{aligned}
&C_1 = (1+m_3)^3 + 2m_3(m_1 - m_2), && C_2 = 2(m_1 - m_2) + (1+m_3),\\
&C_3 = 2(m_1 - m_2) - (1+m_3), && C_4 = (1+m_3)^3 + 2m_3 C_3,\\
&C_5 = (1+m_3)^4 - m_3 C_3^2, && C_6 = 2(1+m_3)^3 + m_3 C_3,\\
&C_7 = m_3(m_1 - m_2) - (1+m_3)^3, && C_8 = 2(m_1 - m_2)(1+m_3) + m_3 C_3,\\
&C_9 = (1+m_3)^4 + 2m_3(m_1 - m_2)C_3, && C_{10} = (1+m_3)^4 - m_3 C_3^2.
\end{aligned} \tag{42}
$$

Next, we briefly explain how to use the method of normal forms to study bifurcation of multiple limit cycles. Suppose the general nonlinear differential system we are considering is given by $\dot{\boldsymbol{x}} = J\boldsymbol{x} + \boldsymbol{f}(\boldsymbol{x})$, where $J\boldsymbol{x}$ and $\boldsymbol{f}(\boldsymbol{x})$ represent the linear and nonlinear parts of the system, respectively. We assume $\boldsymbol{f}$ is analytic and $\boldsymbol{f}(\mathbf{0}) = \mathbf{0}$, implying that $\boldsymbol{x} = \mathbf{0}$ is an equilibrium point of the system, and J is the Jacobian of the system evaluated at the equilibrium point $\boldsymbol{x} = \mathbf{0}$. Further suppose J contains a purely imaginary pair and its other eigenvalues have negative real part. Then, by applying normal form theory, we can obtain the following normal form in the polar coordinates:

$$
\begin{aligned}
\dot{r} &= r\,(v_0 + v_1\,r^2 + v_2\,r^4 + \cdots + v_k\,r^{2k} + \cdots),\\
\dot{\theta} &= \omega_c + \tau_1\,r^2 + \tau_2\,r^4 + \cdots + \tau_k\,r^{2k} + \cdots,
\end{aligned} \tag{43}
$$

where r and θ denote the amplitude and phase of motion, respectively. Both v_k and τ_k are explicitly expressed in terms of the original system's coefficients. v_k is called the kth-order focus value of the Hopf-type critical point (the origin). The zero-order focus value v_0 is obtained from a linear perturbation.

The basic idea of finding k small-amplitude limit cycles of the system $\dot{\boldsymbol{x}} = J\boldsymbol{x} + \boldsymbol{f}(\boldsymbol{x})$ around the origin is as follows: First, find the conditions such that $v_0 = v_1 = \cdots = v_{k-1} = 0$ (note that $v_0 = 0$ is automatically satisfied at the critical point), but $v_k \neq 0$, and then perform appropriate small perturbations to prove the existence of k limit cycles. The following lemma gives sufficient conditions for the existence of small-amplitude limit cycles. (The proof can be found in [Yu & Han, 2005].)

Lemma 2. *Suppose that the focus values of a dynamical system depend on k parameters, expressed as*

$$
v_j = v_j(\epsilon_1,\, \epsilon_2,\, \ldots,\, \epsilon_k), \quad j = 0,\, 1,\, \ldots,\, k, \tag{44}
$$

satisfying

$$
\begin{aligned}
&v_j(0, \cdots, 0) = 0, \quad j = 0,\, 1,\, \ldots,\, k-1, \quad v_k(0, \cdots, 0) \neq 0,\\
\text{and} \qquad &\det\left[\frac{\partial(v_0, v_1, \ldots, v_{k-1})}{\partial(\epsilon_1, \epsilon_2, \ldots, \epsilon_k)}\,(0, \cdots, 0)\right] \neq 0.
\end{aligned} \tag{45}
$$

Then, for any given $\epsilon_0 > 0$, there exist $\epsilon_1,\, \epsilon_2,\, \ldots,\, \epsilon_k$ and $\delta > 0$ with $|\epsilon_j| < \epsilon_0$, $j = 1, 2, \ldots, k$ such that the equation $\dot{r} = 0$ has exactly k real positive roots for r (i.e., the dynamical system has exactly k limit cycles) in a δ-ball with the center at the origin.

Now we apply the Maple program developed in [Yu, 1998] for computing the normal forms of Hopf and generalized Hopf bifurcation to system (41) to obtain

$$
\begin{aligned}
v_1 = &\frac{m_3(1+m_3)^2\left[2(m_1-m_2)+m_3(1+m_3)\right]\left[2m_3(m_1-m_2)+1+m_3\right]}{C_1^2 C_3^2\left[(1+m_3)^3+8m_3(m_1-m_2)\right]\omega_c}\\
&\times\big[\,4m_4 m_1^2 - (m_3^3 + 8m_2 m_3 + 5m_3^2 + 5m_3 + 1)\,m_1\\
&\quad +2(1+m_3)^4 + m_2(m_3^3 + 4m_2 m_3 + 5m_3^2 + 5m_3 + 1)\,\big],\\
v_2 = &\cdots,
\end{aligned}
$$

where C_1 and C_3 are given in (42), and the lengthy expression of v_2 is omitted here for brevity. Eliminating m_2 from the equations $v_1 = v_2 = 0$ yields a solution $m_2 = m_2(m_1, m_3)$ and one resultant R_{12}, which is a function of m_3 only, given by

$$\begin{aligned}R_{12} = &m_3(m_3+1)(m_3^2+4m_3+1)(m_3^2+14m_3+1)\\ &\times(64260m_3^{16}+11622021m_3^{15}+145525211m_3^{14}+938104849m_3^{13}+4533531166m_3^{12}\\ &+16130725479m_3^{11}+40116273317m_3^{10}+69028372739m_3^{9}+82632778940m_3^{8}\\ &+69028372739m_3^{7}+40116273317m_3^{6}+16130725479m_3^{5}+4533531166m_3^{4}\\ &+938104849m_3^{3}+145525211m_3^{2}+11622021m_3+64260).\end{aligned}$$

Thus, $R_{12} = 0$ has no positive solution for m_3, implying that we can not have solutions for $v_1 = v_2 = 0$. The next best possibility is to have $v_1 = 0$, but $v_2 \neq 0$, yielding two small-amplitude limit cycles. Note that using the values of m_1, m_2 and m_3 given in (36) we have $D_H = \frac{829}{718} \approx 1.154596 < 2$, and $v_1 \approx -0.025201$. In order to have solutions for $v_1 = 0$, we solve the factor in the square bracket in the expression of v_1 for m_1 to obtain

$$m_{1\pm} = \frac{1}{8m_3}\Big[m_3^3+8m_2m_3+5m_3^2+5m_3+1 \pm (1+m_3)\sqrt{m_3^4-24m_3^3-46m_3^2-24m_3+1}\Big].$$

It is easy to see that $m_{1\pm} > 0$ under the condition

$$m_3^4-24m_3^3-46m_3^2-24m_3+1 \geq 0 \quad \Longleftrightarrow \quad m_3 \leq 0.038733\cdots \quad \text{or} \quad m_3 \geq 25.817673\cdots.$$

We take $m_3 = 0.035$, $m_2 = 2.25$, and $m_1 = m_{1-} = 5.284315\cdots$, for which $v_1 = 0$ and $v_2 \approx -0.042726$. Thus, by Lemma 2 we can conclude that system (35) can have two small-amplitude limit cycles near the equilibrium solution E_1 due to Hopf bifurcation. Summarizing the above results we have the following theorem.

Theorem 3. *For the dimensionless system* (35)*, when* $2(m_1-m_2) > 1+m_3$*, it has a Hopf critical point at* $D = D_H = \frac{2m_3(m_1-m_2)+(1+m_3)}{2(m_1-m_2)-(1+m_3)}$*. At the critical values,* $(D, m_1, m_2, m_3) = (0.247813\cdots, 5.284315\cdots, 2.25, 0.035)$*, the focus values at the Hopf critical point give* $v_0 = v_1 = 0$*, but* $v_2 < 0$*. Thus, perturbing the parameters* D *and* m_2 *(or* m_1 *or* m_3*) around the critical values yields two small-amplitude limit cycles around the origin.*

Note in Theorem 3 that in order to obtain two limit cycles, the values of D and m_3 are chosen quite smaller than that given in (30). To realize the two limit cycles, we take perturbations on m_1 and D as $m_1 = 5.284315 + \varepsilon_1$, where $\varepsilon_1 = 0.01$, and so the focus values become

$$v_0 = 0, \quad v_1 \approx 0.00002383, \quad v_2 \approx -0.04266341,$$

which indicates that we must choose a perturbation on D as $D = 0.247813 + \mu$ such that $v_0 < 0$. Since at the above parameter values, $\frac{\partial \alpha}{\partial D}(D_H) > 0$, we need to choose $\mu < 0$. Taking $\mu = -0.00001$ yields the following parameter values:

$$D = 0.246971, \quad m_1 = 5.294315, \quad m_2 = 2.25, \quad m_3 = 0.035, \tag{46}$$

under which the focus values become

$$v_0 \approx -0.555332 \times 10^{-6}, \quad v_1 \approx 0.238308 \times 10^{-4}, \quad v_2 \approx -0.042663.$$

Thus, the truncated normal form equation $\dot{r} = v_0 + v_1 r^2 + v_2 r^4 = 0$ yields the solutions for the amplitudes of the two limit cycles: $r_1 \approx 0.154551$ and $r_2 \approx 0.268972$. Since $v_0 < 0$ and $v_2 < 0$, the equilibrium point $E_1 : (X, Y, Z) = (0.292315, 2.441367, 2.441367)$ and the outer limit cycle are stable, while the inner limit cycle is unstable due to $v_1 > 0$. This is indeed a bistable phenomenon consisting of a stable equilibrium and a stable limit cycle. The unstable limit cycle is a separator for the two attracting regions on the center manifold. Trajectories starting from the two regions converge to different attractors, one to the equilibrium, and the other to the limit cycle.

If we change m_2 from 2.25 to 2.8, and choose $\varepsilon_1 = -1.9$ and $\mu = 0.01$, then we have the following parameter values:

$$D = 0.903352, \quad m_1 = 3.934315, \quad m_2 = 2.80, \quad m_3 = 0.035, \tag{47}$$

and the associated focus values are:

$$v_0 \approx 0.988062 \times 10^{-4}, \quad v_1 \approx -0.128829 \quad v_2 \approx 1.664395.$$

Thus, the truncated normal equation $v_0 + v_1\, r^2 + v_2\, r^4 = 0$ yields the solutions for the amplitudes of the two limit cycles: $r_1 = 0.027694$ and $r_2 = 0.652623$. Now for this case, $v_0 > 0$ and $v_2 > 0$, the equilibrium point $\mathrm{E}_1 : (X, Y, Z) = (0.144425,\, 0.595957,\, 0.595957)$ and the outer limit cycle are unstable, while the inner limit cycle is stable because of $v_1 < 0$. Hence, for this case the system does not exhibit bistable phenomenon, and all solution trajectories starting near the equilibrium point converge to the stable limit cycle.

Numerical simulations for these cases discussed above will be given in next section.

5. Numerical Simulations

In this section, numerical simulations are present to compare with the analytical predictions obtained in the previous sections. In particular, the comparison between the analytical and numerical results obtained for the Hopf bifurcation is given. In order to give a good comparison, we fix all parameter values, but α (or μ), which is treated as a bifurcation parameter. The parameter α is varied to show the stable equilibrium solutions E_0 and E_1, and stable limit cycles. Moreover, we will choose a large positive value of μ, which means that this value is far away from the Hopf critical point α_H, to demonstrate the blips phenomenon.

Having taken all parameter values, except for α, from Table 2.1, it follows from Lemma 1 that the equilibrium solution E_0 is asymptotically stable for $0 < \alpha < \alpha_t = 0.2025 \times 10^{-3}$. Then, as α is increased to pass through α_t, E_0 becomes unstable and bifurcates into the equilibrium solution E_1, which is asymptotically stable for $\alpha_t < \alpha < \alpha_H = 0.7867 \times 10^{-3}$. As α is further increased, E_1 becomes unstable at the Hopf critical point $\alpha = \alpha_H$, leading to a family of limit cycles. The normal form obtained for the Hopf bifurcation is given in (27). Since $v_1 = -0.2016072570 \times 10^{-11} < 0$, the Hopf bifurcation is supercritical, and the bifurcating limit cycles are stable.

To show the series of bifurcations, we vary the bifurcation parameter α and increase its value from a small one less than α_t. We first choose $\alpha = 0.15 \times 10^{-3} < \alpha_t$, with the simulation result shown in Figure 2, indicating that E_0 is asymptotically stable, which agrees with the analytical prediction. Next, choose $\alpha_t < \alpha = 0.4 \times 10^{-3} < \alpha_H$, with the simulation result depicted in Figure 3, showing that E_1 is asymptotically stable, which again agrees with the analytical prediction. For $\alpha > \alpha_H$, we select two values of $\mu = 0.3 \times 10^{-11}$ and $\mu = 0.1 \times 10^{-10}$, both of which are near the Hopf bifurcation point, implying two perfect Hopf bifurcations. In order to compare the simulation results with the analytical predictions for the two Hopf bifurcations, we use the sliding and parameter transformation (23), then apply the normal form (27), the limit cycle solutions (29) and (30), and the output (32) from executing the Maple program [Yu, 1998] to obtain the following analytical approximations:

For $\mu = 0.3 \times 10^{-11}$,

$$\begin{aligned}
A(t) = {} & 11.44368258 + 0.46972 \times 10^{-11} \cos(0.70065\, t) + 0.51885 \times 10^{-12} \sin(0.70065\, t) \\
& - 0.83409 \times 10^{-3} \cos(0.23355\, t) + 0.15584 \times 10^{-2} \sin(0.23355\, t) \\
& - 0.46083 \times 10^{-7} \cos(0.46710\, t) - 0.84711 \times 10^{-7} \sin(0.46710\, t), \\
R_n(t) = {} & 48548.88564 + 0.16404 \times 10^{-8} \cos(0.70065\, t) + 0.12499 \times 10^{-7} \sin(0.70065\, t) \\
& - 5.7426 \cos(0.23355\, t) + 0.34563 \times 10^{-8} \sin(0.23355\, t) \\
& + 0.18602 \times 10^{-3} \cos(0.46710\, t) - 0.18823 \times 10^{-3} \sin(0.46710\, t), \\
R_d(t) = {} & 48548.88564 - 0.31754 \times 10^{-8} \cos(0.70065\, t) + 0.13747 \times 10^{-8} \sin(0.70065\, t) \\
& - 2.4296 \cos(0.23355\, t) - 2.8372 \sin(0.23355\, t) \\
& + 0.96927 \times 10^{-4} \cos(0.46710\, t) + 0.38148 \times 10^{-4} \sin(0.46710\, t), \\
E(t) = {} & 12902.43192 + 0.52959 \times 10^{-8} \cos(0.70065\, t) + 0.58498 \times 10^{-9} \sin(0.70065\, t) \\
& - 0.94041 \cos(0.23355\, t) + 1.7570 \sin(0.23355\, t) \\
& - 0.51957 \times 10^{-4} \cos(0.46710\, t) - 0.95508 \times 10^{-4} \sin(0.46710\, t).
\end{aligned} \tag{48}$$

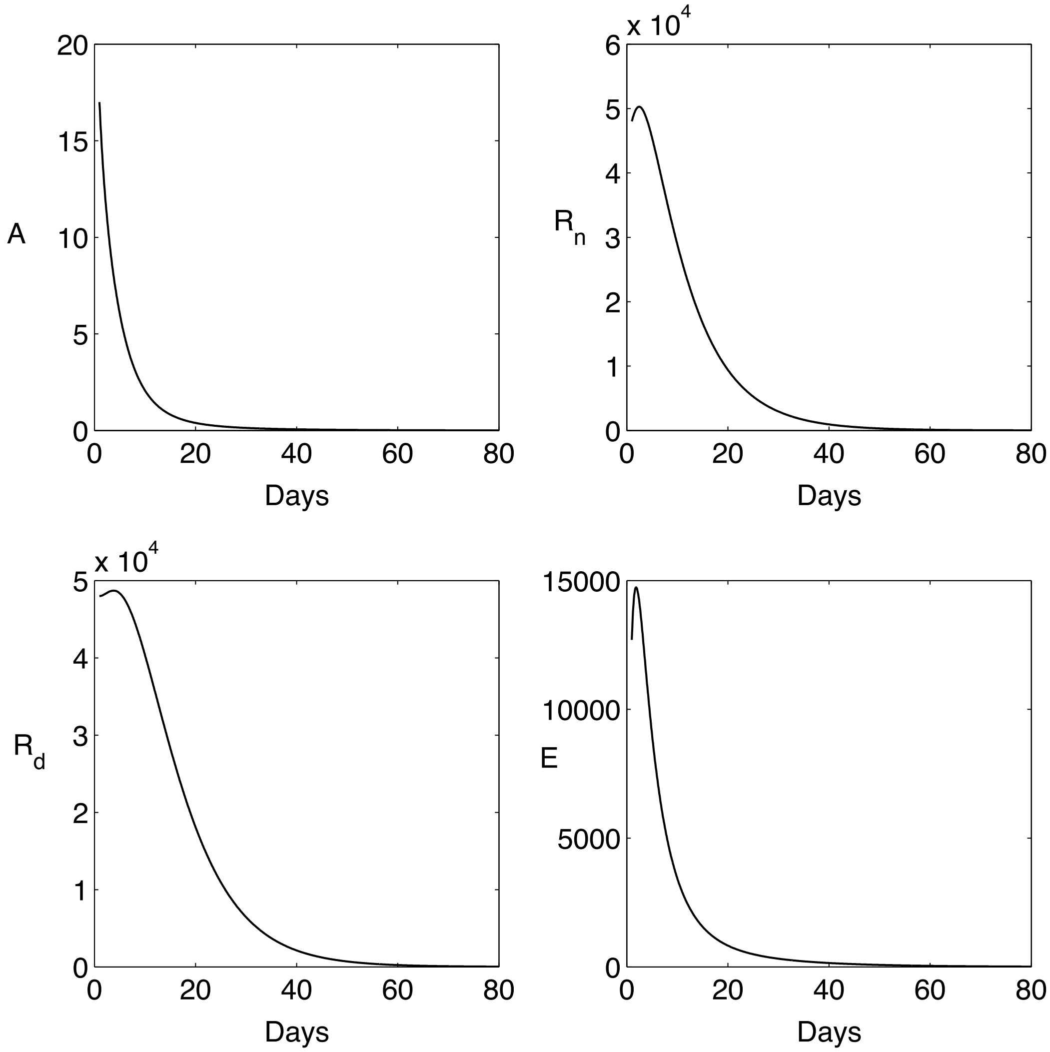

Fig. 2. Simulated time history for system (1) when $\alpha = 0.15 \times 10^{-3} < \alpha_t$, with the initial condition $A(0) = 17$, $R_n(0) = R_d(0) = 48000$, $E(0) = 12700$, converging to E_0.

For $\mu = 0.1 \times 10^{-10}$,

$$\begin{aligned}
A(t) =\ & 11.44368267 + 0.28584 \times 10^{-10} \cos(0.70065\,t) + 0.31574 \times 10^{-11} \sin(0.70065\,t) \\
& - 0.15228 \times 10^{-2} \cos(0.23355\,t) + 0.28452 \times 10^{-2} \sin(0.23355\,t) \\
& -0.15361 \times 10^{-6} \cos(0.46710\,t) - 0.28237 \times 10^{-6} \sin(0.46710\,t), \\
R_n(t) =\ & 48548.88610 + 0.99821 \times 10^{-8} \cos(0.70065\,t) + 0.76060 \times 10^{-7} \sin(0.70065\,t) \\
& - 10.484 \cos(0.23355\,t) + 0.21032 \times 10^{-7} \sin(0.23355\,t) \\
& + 0.62007 \times 10^{-3} \cos(0.46710\,t) - 0.62742 \times 10^{-3} \sin(0.46710\,t), \\
R_d(t) =\ & 48548.88610 - 0.19324 \times 10^{-7} \cos(0.70065\,t) + 0.83652 \times 10^{-8} \sin(0.70065\,t) \\
& - 4.4358 \cos(0.23355\,t) - 5.1798 \sin(0.23355\,t) \\
& + 0.32309 \times 10^{-3} \cos(0.46710\,t) + 0.12716 \times 10^{-3} \sin(0.46710\,t), \\
E(t) =\ & 12902.43196 + 0.32227 \times 10^{-7} \cos(0.70065\,t) + 0.35598 \times 10^{-8} \sin(0.70065\,t) \\
& - 1.7169 \cos(.23355\,t) + 3.2078 \sin(0.23355\,t) \\
& - 0.17319 \times 10^{-3} \cos(0.46710\,t) - 0.31836 \times 10^{-3} \sin(0.46710\,t).
\end{aligned} \tag{49}$$

The two sets of simulation results compared with the above two sets of analytical solutions are shown

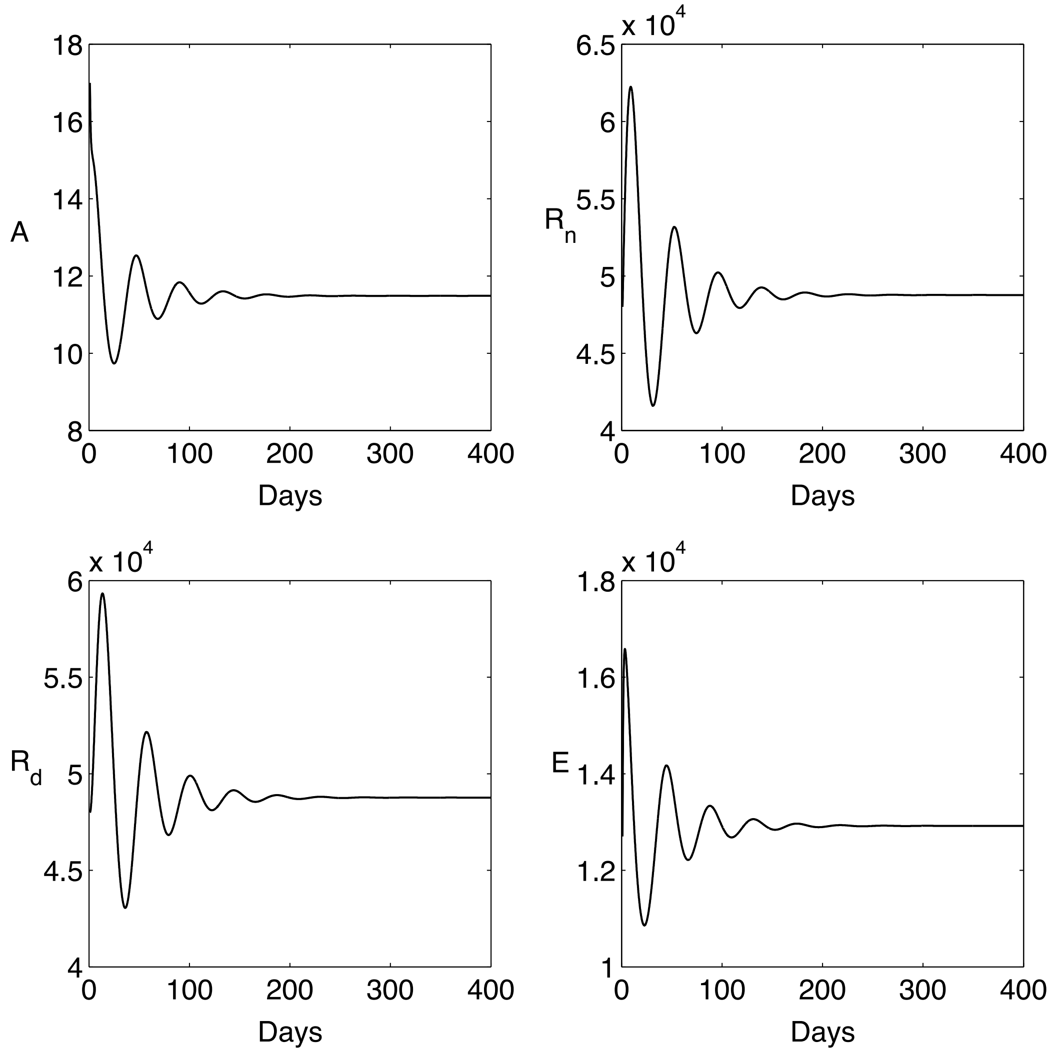

Fig. 3. Simulated time history for system (1) when $\alpha = 0.4 \times 10^{-3}$, with the initial condition, $A(0) = 17$, $R_n(0) = R_d(0) = 48000$, $E(0) = 12700$, converging to E_1.

in Figure 4. It clearly shows a very good agreement between the simulation results and the analytical predictions, particularly for the smaller value of μ, as expected. The comparison result for $\mu = 0.3 \times 10^{-11}$ has been given in [Zhang *et al.*, 2014], but the detailed analytical formulas are not given there. Finally, to demonstrate the blips phenomenon, we choose a value of $\alpha = 0.3 \times 10^{-2} > \alpha_H$, which is not close to α_H, and so the normal form theory is not applicable for this value. The simulation result for this case is given in Figure 5, indeed showing the blips phenomenon. Since the solutions of the system are positive and bounded, and the Hopf bifurcation induces oscillations, we expect that the system can have large-amplitude oscillating solutions (a persistent motion), and choosing appropriate parameter values can tune the frequency of the motion to become blips. The biological reason for the model to exhibit blips is as follows (see Figure 5): the variable E grows very quickly in the absence of the variables R_n and R_d, and then R_n responds very quickly (due to the EA term) and suppresses the E, but the R_n does not last long. This explains how the adaptive and innate immune responses work too, against pathogens. But why is the E not eliminated like a pathogen would be? Maybe because the system is now “torn between two equilibria”.

Finally, we present simulations for the two limit cycles obtained in the previous section. We take the parameter values for the two different cases, given in (46) and (47), and use the normalized system (24) to

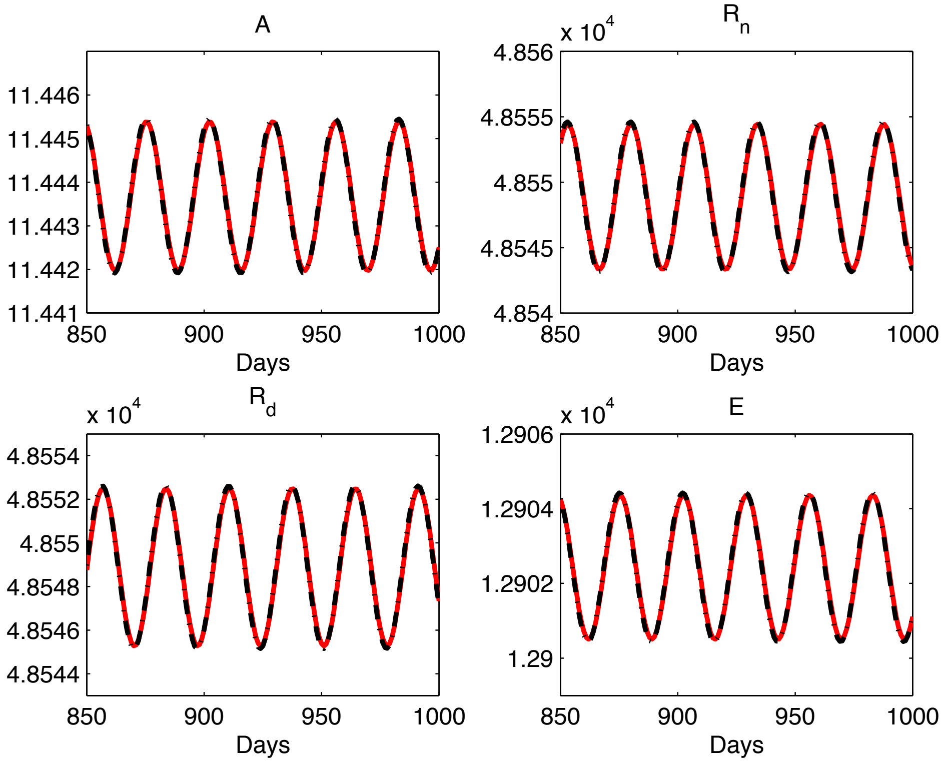

(a)

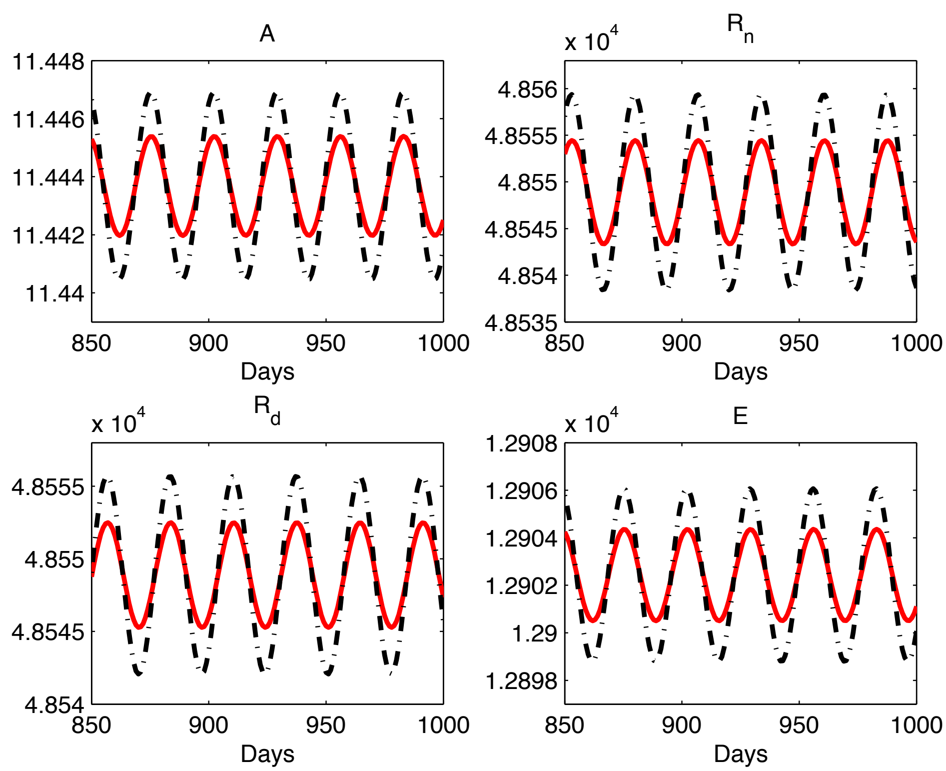

(b)

Fig. 4. Comparison between the simulated time history and analytical approximations for system (1), the red solid line denoting the simulation results, while the black dash-dot line indicating the analytical predictions. The bifurcation parameter values of μ are taken for two cases: (a) $\mu = 0.3 \times 10^{-11}$ and (b) $\mu = 0.1 \times 10^{-10}$, both converging to stable limit cycles.

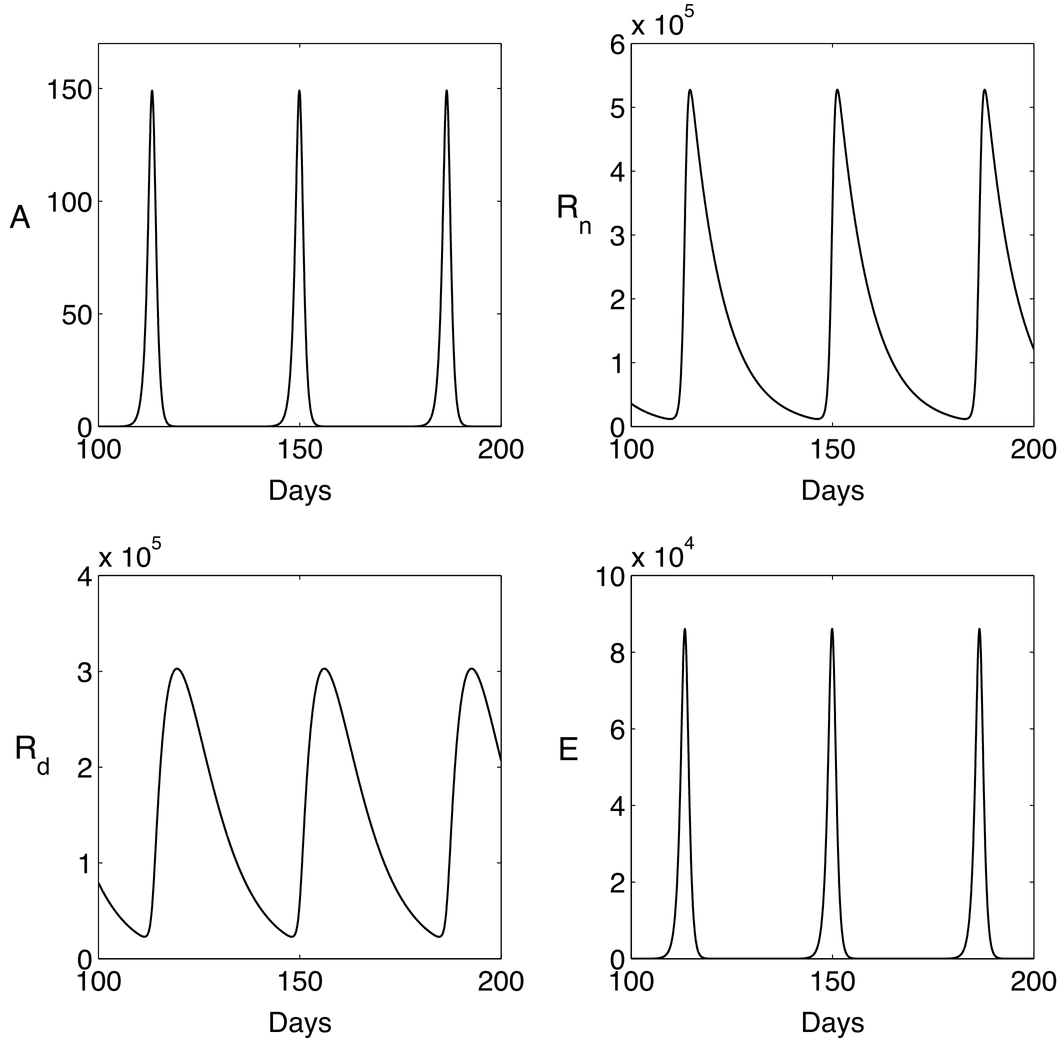

Fig. 5. Simulated time history for system (1) when $\alpha = -0.3 \times 10^{-2}$, showing blips.

perform the simulation. The simulation results are shown in Figures **??** and **??** for the two cases, where ...

6. Conclusion

In this paper, we have given a detailed study on an autoimmune model, particularly for bifurcation and stability properties. The main attention is focused dynamical oscillating behavior of the model, which may lead to the interesting and important phenomenon–blips. After finding two equilibrium solutions and their stability conditions, we have paid particular attention to Hopf bifurcation which may occur from the disease equilibrium, since Hopf bifurcation is a necessary condition to generate blips. We have applied center manifold theory and the method of normal forms to give a detailed analysis on the Hopf bifurcation. We have obtained the exact analytical formulas for the approximate solutions of limit cycles, which are compared with numerical simulations to show a very good agreement between the simulations and the analytical predictions.

Acknowledgment

This work was supported by the Natural Sciences and Engineering Research Council of Canada (No. R2686A02).

References

Alexander, H. K. & Wahl, L. M. [2011] "Self-tolerance and autoimmunity in a regulatory T cell model," *Bulletin of Mathematical Biology*, **73**(1), 33–71.

DeFranco, A., Locksley, R. & Robertson, M. [2007] *Immunity: The Immune Response to Infectious and Inflammatory Disease*, New Science Press Ltd., London, 2007.

Farber, E. M, Mullen, R. H, Jacobs, A .H & Nall, L. [1986] "Infantile psoriasis: a follow-up study," *Pediatric Dermatology*, **3**, 237–243.

Fergusson, D. M., Horwood, L. J. & Shannon, F. T. [1990] "Early solid feeding and recurrent childhood eczema: A 10-year longitudinal study," *PEDIATRICS*, **86**(4), 541–546.

Field, E. H, Kulhankova, K. & Nasr, M. E. [2007] "Natural Tregs, $CD4^+$ $CD25^+$ inhibitory hybridomas, and their cell contact dependent suppression," *Immunologic Research*, **39**, 62–78.

Girschick, H. J., Zimmer, C., Klaus, G., Darge, K., Dick, A. & Morbach, H. [2007] "Chronic recurrent multifocal osteomyelitis: what is it and how should it be treated?" *Nature Clinical Practice Rheumatology*, **3**, ???–???.

Guckenheimer, J. & Holmes, P. [1990] *Nonlinear Oscillations, Dynamical Systems, and Bifurcations of Vector Fields* (3rd Ed.), Springer-Verlag, New York, 1990.

Hinrichsen, D. & Pritchard, A. J. [2005] *Mathematical Systems Theory I: Modelling, State Space Analysis, Stability and Robustnes* (2nd Ed.), Springer-Verlag, New York, 2005.

Iyer, R. S., Thapa, M. M. & Chew, F. S. [2011] "Chronic recurrent multifocal osteomyelitis: review," *American Journal of Roentgenology*, **196**(6 Suppl), S87S91.

Miyara, M. & Sakaguchi, S. [2007] "Natural regulatory T cells: mechanisms of suppression," *Trends in Molecular Medicine*, **13**, 108–116.

Munro, D. D. [1963] "Recurrent subacute discoid lupus erythematosus," *Proceedings of the Royal Society of Medicine*, **56**(2), 78–79.

Sakaguchi, S., Miyara, M., Costantino, C. M. & Hafler, D. A. [2010] "$FOXP3^+$ regulatory T cells in the human immune system," *Nat Rev Immunol*, **10**(7), 490–500.

Scheffold, A., Hühn, J. & Höfer, T. [2005] "Regulation of $CD4^+$ $CD25^+$ regulatory T cell activity: it takes (IL-)two to tango," *European Journal of Immunology*, **35**, 1336–1341.

Scheffold, A., Murphy, K. M. & Höfer, T. [2007] "Competition for cytokines: Treg cells take all," *Nature Immunology*, **8**, 1285–1287.

Yu, P. [1998] "Computation of normal forms via a perturbation technique," *Journal of Sound and Vibration*, **211**(1), 19–38.

Yu, P. [2003] "A simple and efficient method for computing center manifold and normal forms associated with semi-simple cases," *Dynamics of Continuous, Discrete and Impulsive Systems Series B: Applications & Algorithms*, **10**(2), 273-286.

Yu, P. & Han, M. [2005]

Yu, P. [2005] "Closed-form conditions of bifurcation points for general differential equations," *International Journal of Bifurcation and Chaos*, **15**(4), 1467–1483.

"Small limit cycles bifurcating from fine focus points in cubic-order z_2-equivariant vector fields," *Chaos, Solitons Fractals*, **24**, 329–348.

Zhang, W., Wahl, L. M. & Yu, P. [2014] "Modelling and anlysis of recurrent autoimmune disease," *SIAM Journal on Applied Mathematics*, **74**(6), 1998–2025.